UCRL- 1195

C.2

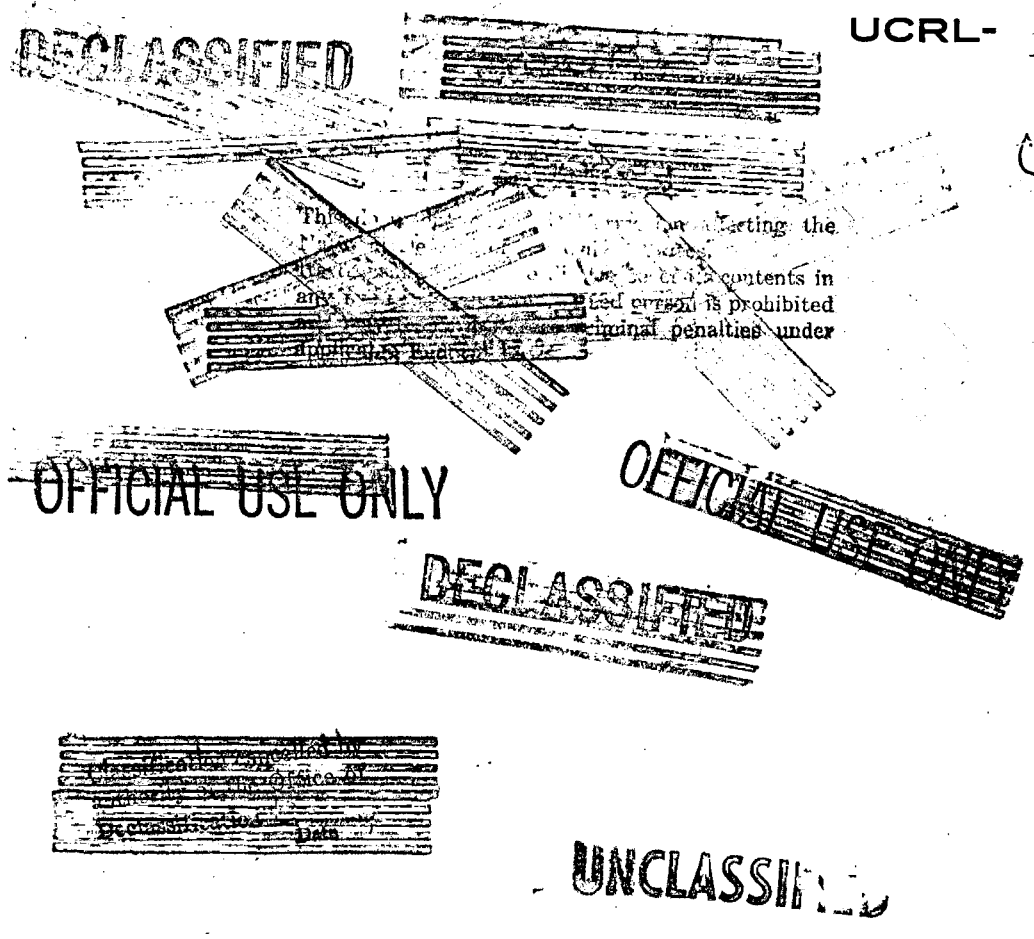

RADIATION LABORATORY

DISCLAIMER

Classification cancelled by authority of the Office of Declassification 12-54 Date

OFFICIAL USE ONLY

4

UNIVERSITY OF CALIFORNIA
Radiation Laboratory

UNCLASSIFIED

Cover Sheet
Do not remove

This document contains information affecting the national defense of the United States within the meaning of the Espionage Act, U.S.C. 50:31 and 32. Its transmission or the revelation of its contents in any manner to an unauthorized person is prohibited by law. Information so classified may be imparted only to persons in the employ of the United States Government who have a need to know such information in connection with their official duties. Persons receiving this document by authority of the contractor or his employees are subject to the applicable penalties of these laws.

INDEX NO. UCRL 1195
This document contains 80 pages
This is copy 8 of 30 Series A

OFFICIAL USE ONLY

Issued to ~~Chem. Div.~~ INFORMATION DIVISION
RADIATION LABORATORY
UNIVERSITY OF CALIFORNIA
BERKELEY, CALIFORNIA

~~CONFIDENTIAL~~ SECRET

classification

Each person who receives this document must sign the cover sheet in the space below.

Route to	Noted by	Date	Route to	Noted by	Date
Templeton	✓	✓			
CHEMISTRY DIVISION					
C. Corvalan					

HIGH ENERGY FISSION. SPALLATION OF URANIUM

Robert Lancaster Folger
B.S. (University of Illinois) 1948

DISSERTATION

Submitted in partial satisfaction of the requirements for the degree of

DOCTOR OF PHILOSOPHY

in

GRADUATE DIVISION

of the

UNIVERSITY OF CALIFORNIA

Approved:

.....

.....

.....
Committee in charge

Deposited in the University Library .....
Date Librarian

TABLE OF CONTENTS

HIGH ENERGY PROTON FISSION - SPALLATION OF URANIUM

Robert Lancaster Folger
Radiation Laboratory and Department of Chemistry
University of California, Berkeley, California

ABSTRACT

The fission and spallation reactions caused in uranium by bombardment with high energy protons (340 to 350 mev) were investigated. The reaction products were separated from the target by chemical processes and identified by their radioactive properties. The relative yields of the observed fission products were measured, and the results plotted as a function of mass number. Several of the spallation products were identified and their yields estimated.

An attempt was made to determine the most probable atomic number for a nuclide of given mass formed directly from fission. Studies were made of the relative yields along several isobaric chains as a function of atomic number. From these data predictions of the mass and charge of the fissioning nucleus are made.

Using the reaction $Al^{27}(p,3pn)Na^{24}$ of known cross section to monitor the bombarding beam, the formation cross sections for several fission product nuclides were measured. Values for these reference nuclides were used to transform the relative yields into formation cross sections. Integration over the range of mass numbers of the area under the curve of formation cross section as a function of mass number led to a value for the total fission cross section for uranium bombarded with high energy protons, assuming predominantly binary fission.

HIGH ENERGY PROTON FISSION - SPALLATION OF URANIUM

Robert Lancaster Folger
Radiation Laboratory and Department of Chemistry
University of California, Berkeley, California

I. INTRODUCTION

A. Summary of Previous Data on High Energy Fission

In recent years there has been considerable interest in the mechanism of fission induced by high energy particles (greater than a few mev) as compared to that of low excitation fission. The greatest amount of work has been done with the target elements bismuth,[1] thorium,[2,3] and uranium.[3,4] High energy fission of other heavy elements from Z = 73 to Z = 82 has been observed.[5] Recently, Batzel and Seaborg[6] have announced the high energy fission of a number of medium weight elements. The yield distribution of fission products has been studied by chemical separation techniques followed by identification of the nuclides through radioactivity measurements, and also by measurement of the kinetic energies of the fission fragments.

The predominant characteristics of high energy fission which appear from these studies are:

(1) A single peak is found in the yield versus mass distribution curve, indicating symmetric fission.

(2) Prefission evaporation of nucleons is evidenced by the mass number of the yield peak being less than one-half the mass of the target nucleus.

(3) The kinetic energies of the fission fragments seem to be practically independent of the initial target nucleus excitation.

Predominantly symmetric fission has been reported by Goeckermann and Perlman[1] (bismuth plus 190 mev deuterons), O'Connor and Seaborg[4] (uranium

plus 380 mev helium ions), and Jungerman and Wright[3] (uranium plus 90 mev neutrons).* At intermediate energies, the contribution of asymmetric fission is shown by the appearance of two peaks with a shallow dip between them. This effect has been observed by Newton[2] (thorium plus 38 mev helium ions), and Jungerman and Wright[3] (uranium plus 45 mev neutrons).*

In the high energy deuteron fission of bismuth, Goeckermann and Perlman[1] observed that the mass of the symmetric peak yield was less than one-half the mass of the target nucleus. The mass difference indicated the evaporation of 10 to 12 nucleons. The relative yields of the fission product isobars seemed to indicate that the most probable primary products were those having the same charge to mass ratio as the fissioning nucleus. Yamaguchi,[7] in a theoretical treatment of nuclear evaporation, has shown that for bismuth bombarded with 200 mev deuterons, the half-width for neutron emission is greater than the half-width for fission until 10 to 11 neutrons have been emitted. In the case of uranium bombarded with 380 mev helium ions,[4] the peak mass was not well enough defined to demonstrate prefission nuclear evaporation although the curve showed a strong possibility that such evaporation had occurred.

Measurements of fission fragment kinetic energies have been made by Jungerman and Wright,[3] using ionization chamber techniques, and indirectly by Douthett,[8] measuring the ranges of the fragments in aluminum. In bombarding uranium with 45 and with 90 mev neutrons, Jungermann[3] observed the mean kinetic energies to be 79 ± 3 and 80 ± 2 mev, respectively. Within the limits of experimental error, the ranges of fission fragments obtained by radiochemical separation from absorber foils were respectively the same for slow neutron fission of U^{235},[9,10] uranium plus 18 mev deuterons,[8] and

---

*Represents ionization chamber measurement of fragment kinetic energies.

uranium plus 335 mev protons.[8]

These results would seem to indicate that the actual fissioning nucleus in each case is in a relatively unexcited state and that the high initial excitation energy is used primarily in the prefission evaporation of nucleons.

B. Statement of the Problem

The purpose of this research was to investigate the fission and spallation reactions caused in uranium by bombardment with high energy protons (340 to 350 mev). The reaction products were separated from the target by chemical processes and identified by their radioactive properties. Measurement was made of the relative yields of the observed fission products and the results plotted as a function of mass number (Fig. 1).

An attempt was made to determine the primary products (those formed directly from fission with highest probability for a given mass) for various mass numbers. An estimate of the location of primary products with respect to the stable nuclides may be made by observing the variation of independent yield with mass for a given element in the region of interest. A more accurate determination of primary products may be made by determining the independent yields (formed directly in fission rather than by growth from a radioactive "parent") of nuclides of a given mass number as a function of atomic number.

In contrast to the case of bismuth[1] the fission instability of the heavy elements in the region of uranium is such that fission is energetically possible at low excitation energies without the necessity of the previous evaporation of large numbers of neutrons to give a favorable Z^2/A parameter. However, at the high excitations obtainable with 340 mev protons, it is possible for many nucleons to be evaporated prior to fission.[1] It is of interest therefore to determine the most probable fissioning nucleus under

these conditions. From the work of O'Connor and Seaborg,[4] the yield versus mass curve might be expected to show a distinct symmetry about a single peak. This would suggest that symmetric binary fission is the most probable mode of fission. Since the most probable fission is symmetric, the mass of the peak of the yield versus mass curve should be one-half the mass of the fissioning nucleus. The ratio Z/A of the primary fission products may be used to determine the atomic number of the fissioning nucleus. Where the Z/A ratio is constant as in the case of bismuth fission,[1] a homogeneous fluid model of the fissioning nucleus may be chosen. When the Z/A ratio is not constant, several statistical nuclear models may be used, some of which involve bound groups within the nucleus.

The excited nuclei formed in the target by the bombarding beam do not necessarily undergo fission. In some cases the evaporation of nucleons may proceed to give spallation products which do not fission. An attempt was made to identify several spallation products and make a rough estimate of their yields in an effort to determine what fraction of the total reactions proceeded by this path.

The cross section for the reaction $Al^{27}(p,3pn)Na^{24}$ was measured by comparing it to the cross section for the reaction $C^{12}(p,pn)C^{11}$ which has been measured by Aamodt, Peterson, and Phillips.[11] By monitoring the bombarding beam with aluminum foils it becomes possible to measure the formation cross sections for several reference mass nuclides. Using these values, the yield versus mass curve could be transformed into a "formation cross section versus mass" curve. Integration under this curve makes possible the determination of the fission cross section for uranium with 340 mev protons, assuming predominantly binary fission.

II. FISSION PRODUCT YIELDS

A. General Considerations

Relative Yields

The fundamental equation of formation of a radioactive species in a thin target where N atoms are exposed to a bombarding beam of intensity I is:

$$dn/dt = IN\sigma - \lambda n \qquad \text{(II-1)}$$

where n represents the number of atoms of radioactive species present at time t, λ is the decay constant, and σ is the cross section for formation. Integration of Equation (II-1) over the duration of the bombardment (assuming a constant beam intensity) gives:

$$IN\sigma = \lambda n/(1-e^{-\lambda t}) \qquad \text{(II-2)}$$

where λn represents the disintegration activity of the species at the end of bombardment and t is the duration of the bombardment. The quantity $IN\sigma$, called the independent rate of formation, R, is independent of the duration of the bombardment and proportional to the cross section for formation of the radioactive species under consideration. R is easily obtained for a given species if the activity of the species at end of bombardment is known (Equation II-2).

For a given bombardment, the independent rates of formation may be related by the expression:

$$\frac{R_1}{R_2} = \frac{\lambda_1 n_1(1 - e^{-\lambda_2 t})}{\lambda_2 n_2(1 - e^{-\lambda_1 t})} = \frac{\sigma_1}{\sigma_2} \qquad \text{(II-3)}$$

since I and N are assumed constant during a particular bombardment. If the absolute cross section for formation of a given species is known, the

formation cross sections for other species isolated from the same bombardment are easily obtained by use of Equation (II-3).

Most of the earlier determinations in this work were made relative to the independent rate of formation of Ba^{140} and its precursors since no absolute formation cross sections had been measured at that time. The initial yield results are therefore expressed relative to the independent rate of formation of Ba^{140} and its precursors, taken arbitrarily to be 1.00. The "relative yield" is defined to be the ratio of the cross section of formation of the nuclide in question to the cross section of formation for Ba^{140} and its precursors.

Chemical Techniques

Determination of the Percent Recovery.-- The final counting sample of a radioactive nuclide does not in general consist of 100 percent of the amount of this species produced in the bombardment (allowing for decay). To correct for the amount of active species lost during the chemical separation procedure, it is customary to mix with the active species a known amount (usually 1 to 10 mg) of the inactive element, called the carrier, whose isotopes are being considered. Precautions must be taken to ensure that the active atoms exchange with the stable atoms of the carrier in such a way that a homogeneous mixture is obtained. Until the time when exchange with the carrier has had an opportunity to proceed to equilibrium, care must be taken that none of the active species is lost by volatilization, spattering, adsorption onto glass, or partial coprecipitation with or adsorption on a compound which is removed from the main body of target material.

Assuming equilibrium exchange, the percent recovery of the active species is assumed to be identical with the percent recovery of the carrier

material. Carrier solutions, usually of the nitrate or chloride salts of the elements to be considered, were made up to an approximate concentration of 10 grams of element desired per liter. The solutions were standardized by conventional analytic procedures, usually gravimetric. The percent recovery was obtained by gravimetric analysis of the final solution obtained in the separation procedure.

In the early work it was customary to evaporate an aliquot of the final solution on a counting plate for the radioactive sample, then precipitate a suitable compound for the gravimetric analysis. In later work it was found desirable to use the final precipitate itself, after weighing, for the radioactive sample (see Section III below). In these cases the final precipitate, after washing, was slurried with a volatile nonsolvent liquid and transferred by pipette to an aluminum dish approximately one inch in diameter weighing between 70 and 80 milligrams. The sensitivity of the balance used was of the order 10^{-2} milligram and the samples usually had a net weight between 1 and 10 milligrams. In contrast to samples dried and weighed on filter paper, samples mounted on aluminum dishes show much greater weight stability since the aluminum does not adsorb moisture from the air.

Separation Techniques.-- In designing a separation procedure it is necessary to consider the estimated radioactive yield of the nuclide desired in relation to the estimated yields of the most likely contaminants. The half-lives of the species involved need be considered because we are interested here in the "counting yield" or relative disintegration activity. For example: A 3 hour activity with one-tenth the formation cross section of a 30 hour activity will in a short bombardment give about the same disintegration activity as the 30 hour activity. Of course, relative counting efficiencies need also be considered in this regard.

In general it is desirable to keep the "counting level" of impurities down to 0.1 percent of each activity sought. This may require chemical purification factors of the order of 10^8. Since a single "specific" step in the chemical procedure may give a purification of only 10^2 or 10^3, it is often necessary to repeat portions of the procedure in order to obtain the desired purity.

The two principal methods of separating the desired element are (1) To selectively remove the element from the contaminants by precipitation (the major radioactive contaminants are diluted by addition of inert "holdback" carriers of their elements so that contamination by adsorption is minimized); solvent extraction and/or distillation (unwanted materials sometimes may be held back by adding agents to form complexes which do not extract or distill under the same conditions as the desired element); adsorption and elution (usually in connection with ion exchange resin); and (2) To remove the contaminants from the desired element by precipitation (scavenges), solvent extraction, or distillation. In practice no single technique usually suffices, but a combination of the above methods is generally employed.

Counting Techniques and Corrections

Measurements.-- Measurements were made of the quanta (both particulate and electromagnetic) emitted by the radioactive sample. That fraction of the emitted quanta passing into the sensitive volume of the detecting instrument which causes a reaction in the detecting instrument is defined to be the "counting efficiency" of the type of quantum under consideration.

Immediately after the reaction in the detecting instrument caused by passage of a quantum, there is a short interval ("dead time") during which the instrument is insensitive to further events. The number of events undetected because of occurrence within the "dead time" is referred to as

the "coincidence loss." As the rate of occurrence of events increases, the probability that an event will follow another within the "dead time" interval and so be undetected also increases. The "coincidence factor" is the percent loss per thousand counts per minute recorded.

The recorded activity of a sample may be increased by the detection of events which did not originate within the sample. Such a "background" may be caused by cosmic rays, local contamination of the counting chamber, a strong radioactive source other than the sample near the counting chamber, or electronic disturbances. The activity recorded by the instrument with no sample present is determined over a period commensurate with the counting period of the sample. This figure is the "background correction."

The "observed counting rate," A_T, counts per minute, is defined to be the recorded counting rate corrected for coincidence loss and background count. After standardization (cf. below), the observed counting rate usually was plotted on semilogarithmic graph paper against time on the linear scale.

Small daily fluctuations occur within the detecting and recording circuits. These may be measured by counting the beta particles from UX_2 in equilibrium with a fixed amount of uranium. An arbitrary value of the "observed" counting rate of this "permanent" sample is selected as the "standard" value of the sample. By comparing the "observed" counting rate of the fixed uranium sample with its "standard" value, it is possible to standardize the other counting rates measured during that period so as to eliminate nonrandom errors.

Detecting Instruments.-- Alpha emitting samples were measured either in a proportional counter or in an ionization chamber instrument. Coincidence losses in these instruments are small but electronic disturbances may be serious. Alpha energies were determined by means of an alpha pulse analyzer.[12]

Samples emitting beta and gamma radiation were counted by means of end-window Geiger-Müller tubes. When this work was begun, the tubes available were of the argon-alcohol type. The chief advantage of this tube was its relatively thin window, usually 2.7 to 3.4 mg/cm^2. These tubes, however, had an average total lifetime of only 10^7 to 10^9 counts. (Tubes required replacement at intervals between two and six months depending on the work load.) Another disadvantage was the high coincidence factor, approximately 1.2 percent per thousand counts per minute. Due to changes in the characteristics of the tubes and the high coincidence loss, counting rates higher than 10,000 counts per minute could not be reliably measured.

For the more recent work, end-window tubes filled with a mixture of argon and chlorine were used. These tubes (Amperex Type 100C, obtainable from Amperex Electronic Company, New York, N. Y.) have a window thickness of 3.5 mg/cm^2. These tubes show greater stability of counting characteristics than the argon-alcohol tubes, and are capable of measuring counting rates a factor of ten higher than the argon-alcohol tubes could measure. The coincidence loss at rates of 100,000 counts per minute is of the order 45 percent or 0.45 percent per thousand counts per minute. Although the 45 percent correction required may seem high, it has been found that the correction factors are reproducible to within the statistical error of the counting. The coincidence factor itself is only about one-third that of the argon-alcohol tubes. A disadvantage of the Amperex tubes is the reduced counting efficiency which is only about 45 percent that of the argon-alcohol tubes for most beta and gamma radiation.[13]

Backscattering.-- Correction factors for the scattering of beta particles into the counter from the backing material on which the sample is mounted have been empirically determined by several workers.[14-16] The

amount of backscatter depends primarily upon the thickness and atomic number of the backing material. The scattering is relatively insensitive to beta energy in the range 0.6 to 3 mev.[15,16] In most of our work, the sample considered and the Ba^{140} monitor were mounted on similar backings so that for relative yields the backscattering correction cancelled out.

Self-Scattering and Self-Absorption Corrections.-- Since the radioactive samples in many cases were of finite mass, it was necessary to determine the loss or gain of apparent activity in passing through the mass of the sample. There is a loss of apparent activity due to absorption in the material of the sample. Scattering of beta particles and electrons by the material of the sample causes an apparent increase in the activity. Some preliminary experiments were performed to determine empirically the combined self-absorption and self-scattering corrections.[17,18] The absorbing power of sample material for particles increases only slowly with the atomic number, but the scattering power increases markedly. In some cases the scattering effects were so great that a net increase in apparent counting rate was obtained even for several milligrams per square centimeter of sample thickness.

Air-Window Absorption.-- The loss of activity by absorption in the air between the sample and the counter window, and in the window itself was determined by straight line extrapolation of aluminum and/or beryllium absorption curves whose initial portions were carefully measured using thin absorbers.

Counting Efficiencies.-- In determining yields of various nuclides it was necessary to make some assumptions regarding relative counting efficiencies. For beta particles and electrons a counting efficiency of 100 percent was assumed. The calculated counting efficiencies for

electromagnetic radiation, based on absorption in the gas of the counter tube, were 0.5 percent for energies from 20 kev to 0.5 mev, and 1 percent per mev thereafter for argon filled tubes.[19] The ratio of the over-all efficiency of the argon-chlorine (Amperex) tubes to the argon-alcohol tubes for the same geometry was determined to be 45 percent by counting a number of samples having beta and electromagnetic radiations of various energies.[13]

Effective Geometry.-- The effective geometry is a term relative to the solid angle subtended by the sensitive volume of the counter tube at various distances from the sample. The sample holders used in the Geiger counting had five positions varying from 0.3 cm from the tube window to 6.7 cm from the tube window. An attempt was made to count the monitor sample in the same position as the sample of the nuclide whose relative yield was being determined. Where such an arrangement was not practical initially, due to too great a difference in the counting rates of the samples, the "geometry" ratio would be determined empirically when the counting rates were more nearly equal. This ratio was not a true geometric ratio alone because of increased air absorption at greater distances from the counter window. In cases where the absorption characteristics of a particular beta were rather well known, measurements of the true geometric ratios between various positions were made.

Treatment of Results

The Decay Factor.-- The activity of a particular nuclide at the moment of cessation of bombardment of the target usually was determined by graphical back-extrapolation of the semilogarithmic activity versus time plot to that moment. In some cases where the half-life of the activity was rather well known and it was not convenient to make the graphical extrapolation, the initial activity was determined analytically from the integrated

decay equation:

$$A_o = A_t\, e^{\lambda t} \qquad \text{(II-4)}$$

where A_o represents the initial activity, A_t represents the activity at time t, and λ is the decay constant.

Resolution of Multicomponent Decays.-- Where a decay curve consists of several components, simple, straight line extrapolation of any single activity may not be immediately obvious: In the simpler cases (two to three components), it was customary to follow the decay until the longest lived component showed straight line decay on a semilogarithmic plot. This activity was then back-extrapolated and subtracted from the original curve. The difference was plotted and the procedure repeated as necessary until all of the components had been resolved.

When two components have half-lives and counting yields of the same order of magnitude, graphical resolution by the above method may be quite difficult. An analytical treatment of the data affords a method of resolving the two components.[20] Consider the observed activity, A to be composed of two components A_1 and A_2 whose half-lives are known.

From the integrated decay Equation (II-4):

$$A = A_1 + A_2 = A_1{}^o e^{-\lambda_1 t} + A_2{}^o e^{-\lambda_2 t} \,. \qquad \text{(II-5)}$$

Multiplying through by $e^{\lambda_1 t}$ we obtain

$$A_e{}^{\lambda_1 t} = A_1{}^o + A_2{}^o e^{(\lambda_1 - \lambda_2)t} \,. \qquad \text{(II-6)}$$

This equation is of the form $y(t) = k + mx(t)$. A plot of $A_e{}^{\lambda_1 t}$ versus $e^{(\lambda_1 - \lambda_2)t}$ should give a straight line whose slope is the initial activity of component 2 and whose intercept is the initial activity of component 1.

Multicomponent decay curves may often be reduced to the simple type discussed above by observing the decay through various absorbers chosen so as to block out or materially reduce the radiations of one or more components.

Decay Chains - The Growth Factor.-- Cases are often encountered in which an unstable species decays to a second unstable species whose activity is also measured. In cases where the half-lives bear the proper ratio to each other, a definite increase can be observed in the activity. From the decay laws it is possible to obtain an expression for the activity of the parent, a_1, in terms of the equilibrium activity, a, and the half-lives T_1 and T_2 of the two species:

$$a_1 = \frac{a(T_1-T_2)}{2T_1-T_2} \qquad \text{(II-7)}$$

where $T_1 > T_2$. This expression, however, assumes that the two species count equally effectively. Such a situation is most often not the case. The "counting probability," k, for a species may be defined as the ratio of the observed counts to the number of counts which would be observed if there were no absorbing material between the sample and the sensitive volume of the tube, and each disintegration at 100 percent geometry gave rise to one count. The relation between the disintegration activity at a given geometry and the observed counting rate is then: $A = ka$. Knowing the counting probabilities and half-lives of parent and daughter, the disintegration activity of the parent is given by:

$$a_1 = \frac{A(T_1 - T_2)}{(k_1 + k_2)T_1 - k_1T_2} \; . \qquad \text{(II-8)}$$

The Saturation Factor.-- (cf., page 8.) Since the duration of bombardment varied from 2 minutes to 14 hours, it was necessary to relate the

counting yields to the cross section of formation by correcting for the decay of the species during the bombardment. As shown above, the activity at end of bombardment is related to the formation cross section by the factor $(1 - e^{-\lambda t})$. It can be seen that for bombardments of infinite length (i.e. "saturation bombardments") the activity at end of bombardment is directly proportional to the formation cross section.

B. Observed Nuclides of the Light Elements:

Z = 25 to Z = 37

Chemical Separation Procedures

Manganese.-- From a nitric acid solution of the uranium target, manganese dioxide was precipitated by the addition of potassium bromate. The precipitate was dissolved in dilute nitric acid containing hydrogen peroxide. Concentrated nitric acid was added and the manganese oxidized to permanganate by the addition of sodium bismuthate. After centrifuging to bring down the excess bismuthate (insoluble), the supernatant was decanted and the permanganate reduced by the addition of oxalic acid. Silver chloride was precipitated to remove any acid insoluble compounds not brought down on the excess sodium bismuthate. The supernatant was diluted and members of the acid sulfide group were precipitated by the addition of hydrogen sulfide gas. The supernatant was made basic and manganous sulfide precipitated. The sulfide was dissolved in nitric acid and the foregoing procedure repeated for additional purification. After dissolving the sulfide from this second cycle, manganese dioxide was precipitated and the manganese determined as Mn_3O_4 after ignition.

Iron.-- Iron carrier in an aqua regia solution of the target (containing the minimum amount of nitric acid) was boiled with concentrated

hydrochloric acid to remove most of the nitrate. The material was taken up in 9 N hydrochloric acid and the iron extracted into di-isopropyl ether. After thoroughly washing the ether layer with 7.5 N hydrochloric acid, the iron was re-extracted into water.* The aqueous solution was acidified to 1 N in hydrochloric acid and antimony and tellurium sulfides precipitated. Ferric hydroxide was precipitated with ammonia gas using barium and strontium "holdback" carriers. The precipitate was dissolved in hydrochloric acid, ruthenium carrier added, and the solution fumed with perchloric acid. Ferric hydroxide was reprecipitated with ammonia and dissolved in nitric acid. Niobium oxalate complex was added and niobium pentoxide precipitated. Barium sulfate and silver iodide were also precipitated to remove radioactive impurities. Ferric hydroxide was reprecipitated with ammonia and dissolved in 3 N nitric acid. Hydrofluoric acid was added and barium fluozirconate precipitated. Ferric hydroxide was precipitated from the supernatant and dissolved in 9 N hydrochloric acid for extraction with di-isopropyl ether. Upon re-extraction into water, the iron was precipitated with ammonia. The hydroxide was washed and ignited, and the iron determined as Fe_2O_3.

Cobalt.-- The acidic target solution containing cobalt carrier was made strongly ammoniacal. The supernatant was removed and the precipitate washed twice with hot aqueous ammonia. From the combined supernatant and washings, ferric hydroxide and barium and strontium carbonates were precipitated. The supernatant was acidified with hydrochloric acid and the acid sulfide group contaminants removed by precipitation with hydrogen sulfide gas.

---

*It was recently found that the yield of iron was materially increased by re-extraction into an acetic acid-sodium acetate buffer solution instead of into water.

The solution was made basic and cobalt sulfide precipitated. The sulfide was dissolved in concentrated nitric acid which was then diluted for precipitation of silver chloride. The supernatant was made basic with potassium hydroxide to precipitate cobalt hydroxide. This was dissolved in 2 to 3 N acetic acid. Nickel "holdback" carrier was added and potassium cobaltinitrite precipitated. The precipitate was dissolved in concentrated hydrochloric acid and the procedure repeated beginning with the ferric hydroxide - alkaline earth carbonate precipitations. The second cobaltinitrite precipitate was dissolved as before and potassium cobaltinitrite reprecipitated. This final precipitate was washed, dried at 110°C and cobalt determined as $K_3Co(NO_2)_6 \cdot H_2O$.

Nickel.-- The acidic target solution containing nickel carrier was made strongly ammoniacal. The supernatant was removed and the precipitate washed twice with hot aqueous ammonia. From the combined supernatant and washings, ferric hydroxide and barium and strontium carbonates were precipitated. The solution was boiled gently to remove some of the excess ammonia, and dimethylglyoxime added to precipitate the nickel. The precipitate was dissolved in concentrated nitric acid which was then diluted to approximately 1 N. Copper, palladium, and antimony sulfides were precipitated several times. The supernatant was boiled to remove excess hydrogen sulfide, then made basic with ammonia gas. Ferric hydroxide was precipitated again. The supernatant was made 0.5 N in hydrochloric acid and palladium dimethylglyoxime was precipitated. The supernatant was neutralized and nickel dimethylglyoxime precipitated. After reprecipitation and washing, the nickel dimethylglyoxime was dried at 110°C and weighed as such.

Copper.-- The acidic target solution containing copper carrier was made strongly ammoniacal. The supernatant was removed and the precipitate

washed twice with hot aqueous ammonia. From the combined supernatant and washings, ferric hydroxide was precipitated. A 5 percent solution of sodium thiocyanate and sodium sulfite was added to the supernatant and it was acidified with glacial acetic acid, after "holdback" carriers of the ammonia complex group elements had been added. The cuprous thiocyanate precipitate was dissolved in a minimum amount of concentrated nitric acid and the solution made 2 N in hydrochloric acid. Cadmium, yttrium, and strontium "holdback" carriers were added, and copper precipitated as the sulfide. The cupric sulfide was dissolved in concentrated nitric acid which was diluted to approximately 4 N for the precipitation of silver chloride. The supernatant was buffered with ammonium hydroxide - sodium acetate, and copper thiocyanate again precipitated. The precipitate was washed, dried at 110°C, and copper determined as CuCNS.

Zinc. The nitric acid solution of the target was diluted to approximately 1 N and zinc mercurithiocyanate precipitated in the presence of oxalic acid. The precipitate was dissolved in 4 N nitric acid, the solution was diluted and the zinc mercurithiocyanate reprecipitated twice. The precipitate was redissolved, the solution diluted, and copper, silver, tin, antimony, and bismuth sulfides precipitated. The supernatant was buffered with ammonium acetate, and zinc sulfide precipitated. The precipitate was dissolved in concentrated hydrobromic acid and evaporated to dryness several times with bromine-hydrobromic acid to remove selenium. The residue was taken up in 1 N sodium hydroxide to which sodium carbonate had been added. Ferric hydroxide and barium and strontium carbonates were precipitated from this solution. The supernatant was acidified to 1 N in hydrochloric acid. Zinc mercuric thiocyanate was precipitated, washed, dried at 110°C and weighed as such. The gravimetric factor was determined empirically.

[N.B. A better sample for counting purposes may be obtained by dissolving the final zinc mercurithiocyanate precipitate, removing the mercury by precipitating it as mercuric sulfide, neutralizing to methyl orange endpoint, and precipitating zinc ammonium phosphate at about 80°C. The precipitate is dried at 105°C and weighed as $Zn(NH_4)PO_4$].[21]

Arsenic.-- The nitric acid solution of the target was boiled nearly to dryness. (N.B. A more recent method removes the nitrate by boiling with formic acid.)[22] The residue was taken up in 6 N hydrochloric acid, a crystal of ammonium iodide added, and arsenic and germanium sulfides precipitated at ice temperature. The sulfides were washed with 6 N sulfuric acid saturated with hydrogen sulfide. The sulfides were dissolved in concentrated ammonium hydroxide. The solution was washed into a glass still, and tellurium, antimony and tin "holdback" carriers added. Concentrated hydrochloric acid was added and germanium tetrachloride was distilled from the solution in a stream of chlorine gas. Hydrogen chloride gas was passed into the residue to remove the chlorine. Cuprous chloride was added to reduce the arsenic to arsenic(III), and arsenic trichloride was distilled from the solution in a stream of hydrogen chloride. The arsenic trichloride was trapped in concentrated hydrochloric acid at ice temperature. Arsenic(III) sulfide was precipitated from the distillate by the addition of hydrogen sulfide gas. The sulfide was dissolved in concentrated ammonium hydroxide, tellurium, antimony, and tin carriers added, and the arsenic trichloride distilled from hydrochloric acid as above. Arsenic(III) sulfide was again precipitated from the distillate and dissolved in concentrated ammonium hydroxide. The solution was acidified with concentrated hydrochloric acid and arsenic(III) sulfide precipitated with hydrogen sulfide. The precipitate was washed, dried at 110°C, and arsenic determined as As_2S_3.

Selenium.-- The uranium target was dissolved under reflux in hydrobromic acid containing bromine, and selenium and tellurium carriers. After solution was complete, the reflux column was replaced by a still head and selenium tetrabromide distilled into bromine water kept at ice temperature. After completion of the distillation, an equal volume of concentrated hydrochloric acid was added to the bromine water at ice temperature, and sodium bisulfite added to reduce the selenium to the red allotropic modification of the zero valence state. After washing, the selenium was dissolved in hydrobromic acid containing bromine and tellurium "holdback" carrier, and redistilled. The reduction and distillation were repeated. The selenium from the final reduction was washed with water and dried with ethanol and diethyl ether. The precipitate was then dried at 110°C and selenium determined as Se.

Bromine.-- The uranium target was dissolved under reflux in nitric acid containing a known amount of freshly precipitated silver bromide (to prevent loss of bromine by volatilization). Exchange of the radioactive bromine or bromide ions with the inert bromide of silver bromide is presumed to be rapid and complete.[23] After separation from the target solution, the silver bromide was washed well and metathesized to silver sulfide in ammoniacal solution. The supernatant was carefully acidified to 1 N in nitric acid, allowing the excess hydrogen sulfide to escape. Iodide carrier was added, oxidized to iodine with 0.1 M sodium nitrite, and extracted into carbon tetrachloride. The iodine extraction was repeated twice. The bromide was then oxidized to bromine by potassium permanganate and extracted into carbon tetrachloride. The organic phase was washed with 1 N nitric acid containing permanganate. The carbon tetrachloride was stirred with water and sodium bisulfite solution added until the bromine had been

reduced to bromide (and consequently gone into the aqueous phase). The bromide was then precipitated by the addition of silver nitrate, washed, dried at 110°C, and weighed as AgBr.

Rubidium.-- An aliquot of the nitric acid solution of the target containing cesium and rubidium carriers was evaporated to fuming with perchloric acid. After cooling, absolute ethanol was added and the solution stirred at ice temperature. The cesium and rubidium perchlorates were washed with absolute ethanol and dissolved in 0.2 N hydrochloric acid. Silver chloride was precipitated, then tellurium, ruthenium, tin, antimony, and silver sulfides. The solution was made basic with sodium hydroxide, and lanthanum, cerium, yttrium, iron, zirconium, and niobium precipitated. Barium and strontium carbonates were then precipitated. The series of sulfide, hydroxide and carbonate precipitations was repeated several times. The final supernatant was evaporated to fuming with perchloric acid. The perchlorates were washed with absolute ethanol, dissolved, and reprecipitated. The perchlorates were then dissolved in 6 N hydrochloric acid and the cesium precipitated with silicowolframic acid. (For further purification of cesium see page 33 below.) More cesium carrier was added to the supernatant and cesium silicowolframate again precipitated. The supernatant was evaporated to near dryness. Chloroplatinic acid and ethanol were added to precipitate rubidium chloroplatinate. The precipitate was washed with ethanol, dried at 110°C and rubidium determined as Rb_2PtCl_6.

Identification of Radioactive Nuclides

Manganese.-- In the manganese fraction separated after an eight hour bombardment of a uranium target, a 5.8 day activity was observed. The absorption characteristics and half-life corresponded to those observed

for Mn^{52} formed by spallation of iron with 340 mev protons.[24] The amount of Mn^{52} produced could be accounted for by the known amounts of iron and nickel impurities in the uranium target.

Iron.-- The iron decay measurements showed two major components. One was the expected 46 day Fe^{59}.* The shorter component, having a half-life of about 8.4 hours, seems to be a new activity. Decay measured through 222 mg/cm^2 of aluminum (to block the particulate radiation of Fe^{59}) showed the 8.4 hour activity. No growth was observed (limit detectable, 20 minutes).

Aluminum absorption measurements of the 46 day activity showed the soft beta radiation of Fe^{59}. Aluminum absorption measurements on the 8.4 hour activity showed a beta particle of about 1.5 mev energy. The sample was measured on a crude magnetic beta ray spectrometer. The 8.4 hour activity showed negative beta radiation. No positrons were observed.

Cobalt.-- Decay measurements of the cobalt fraction showed a component of 1.7 hours. Aluminum absorption measurements of the 1.7 hour activity showed a beta energy of about 1.3 mev.

Nickel.-- The decay of nickel showed components of 2.6 hours and 56 hours, presumably Ni^{65} and Ni^{66}, respectively. Aluminum absorption measurements of the 56 hour Ni^{66} showed the 2.9 mev beta particle of 4.3 minute Cu^{66} in equilibrium.

Copper.-- Three isotopes of copper were identified. 3.4 hour Cu^{61} was observed by following the decay of its positrons on a crude beta ray spectrometer. The 12.9 hour Cu^{64} was also seen in this manner as well as

---

*Unless otherwise indicated, values of the half-life and beta energy for the various nuclides were obtained from either the "Table of Isotopes"[25] or the "Chart of the Nuclides."[26]

by resolution of the decay curve obtained with a conventional Geiger counter. 60 hour Cu^{67} was clearly seen in the beta decay curve.

Fermi-Kurie plots of the crude beta spectrometer positron data showed the 1.2 mev β^+ of Cu^{61} and the 0.66 β^+ of Cu^{64}. Aluminum absorption measurements, taken after the 12.9 hour activity had decayed out, showed the 0.6 mev β^- of Cu^{67}.

Zinc.-- Decay of the zinc samples showed a half-life of 49 hours. A 14 hour growth was observed, indicating the presence of 49 hour Zn^{72} with 14 hour Ga^{72} daughter.

Arsenic.-- Decay of the arsenic samples through 350 mg/cm^2 of aluminum (to block the particulate radiation of As^{77}) showed an activity of 26.8 hours half-life. Decay without absorber showed the 40 hour line of As^{77}.

Selenium.-- The predominant activity in the selenium samples was the 59 minute Se^{81m} with the 17 minute Se^{81} in equilibrium. It was possible to detect the 25 minute Se^{83} both by resolution of the decay curve and by observing the 2.4 hour Br^{83} daughter in the decay measurements. Twenty-four hours after bombardment, the decay curve showed essentially no activity other than the 2.4 hour Br^{83}.

Aluminum absorption measurements on the 59 minute activity showed the 1.5 mev beta particle of Se^{81} (a 17 minute β^- activity formed by isomeric transition of Se^{81m}).

Bromine.-- The bromine decay curves showed mainly 2.4 hour and 35 hour components when measured without absorber. Decay measured through 490 mg/cm^2 of aluminum showed components of 4.4 hour and 34 minute after subtraction of a 35 hour component due to the penetrating radiation of Br^{82}. Decay measured through 750 mg/cm^2 of aluminum showed components of 34 minute and a residium of 4.4 hour and 35 hour activities. The relative counting

efficiency of the 4.4 hour activity was considerably reduced by the increased absorber. Aluminum absorption measurements of the 2.4 hour activity showed a 1 mev beta particle.

From the evidence we conclude that Br^{80m}, Br^{82}, Br^{83}, and Br^{84} are formed as fission products with Br^{83} being produced in highest yield.

Rubidium.-- The rubidium sample showed an activity of 19.5 day half-life, presumably Rb^{86}. The sample was not isolated soon enough to detect any of the shorter lived rubidium isotopes. Aluminum absorption measurements on the rubidium activity showed a 1.8 mev beta particle.

C. Observed Nuclides from Z = 38 to Z = 56: The "Peak Yields"

Chemical Procedures

Strontium.-- The target was dissolved in a minimum volume of concentrated nitric acid containing carriers of the elements to be isolated. After solution was complete, red fuming nitric acid was added and the tube chilled in an ice bath. The precipitate, containing the nitrates of strontium, barium, and coprecipitated radium, was centrifuged and the supernatant decanted. The nitrates were dissolved in a minimum amount of warm water and reprecipitated with fuming nitric acid. The nitrates were redissolved and the solution made 4 N in nitric acid. Silver chloride was precipitated to remove acid insoluble materials which might have been carried by the alkaline earth nitrates. The supernatant was made basic with ammonia gas and ferric hydroxide precipitated to remove traces of ammonium hydroxide group impurities and any insoluble material which might have remained in the solution. The supernatant was buffered to pH 5 with acetic acid-ammonium acetate. Barium chromate (carrying radium) was separated from the strontium by precipitation at 95°C. Barium chromate was again precipitated from the

supernatant in order to remove any traces of radioactive barium or radium. Strontium was precipitated as the carbonate, washed, dissolved in hydrochloric acid to remove carbon dioxide, and reprecipitated as the oxalate for weighing.

Zirconium.-- The nitric acid solution of the target containing zirconium carrier was made about 4-5 N in nitric acid and about 8 N in hydrofluoric acid. Lanthanum and yttrium fluorides were precipitated twice to remove contaminants of the rare earth and actinide series. Barium was added to the supernatant to precipitate barium fluozirconate. The precipitate was dissolved in 8 N nitric acid saturated with boric acid. The foregoing precipitations were repeated for additional purification. The final $BaZrF_6$ precipitate was dissolved in approximately 3 N hydrochloric acid with boric acid added to complex the fluoride. The barium was removed by precipitation as barium sulfate. The supernatant was diluted to approximately 2 N in acid and the zirconium precipitated by 6 percent cupferron solution in the cold (ice bath). The precipitate was washed with the reagent, transferred to a porcelain crucible, ignited and weighed as ZrO_2. This procedure probably effects no separation from hafnium. However, the yield of hafnium isotopes is less than 10^{-3} that of the zirconium.

Niobium.-- Niobium carrier, complexed with oxalate, was added to a measured fraction of the target solution. Niobium pentoxide was precipitated by digesting in an 8 N nitric acid solution containing potassium bromate. The oxide was dissolved in saturated oxalic acid. The solution was taken up in 6 N hydrochloric acid and extracted with cupferron into chloroform at 5°C. The aqueous phase was re-extracted and the combined chloroform layers washed with cold 6 N hydrochloric acid containing cupferron. The chloroform layer was boiled with concentrated nitric acid and potassium

bromate added to precipitate niobium pentoxide. The oxide was dissolved in dilute nitric acid containing hydrofluoric acid. Barium fluozirconate was precipitated to remove zirconium, yttrium, and lanthanide contaminants. Boric acid was added to complex the fluoride, and niobium pentoxide was precipitated from strongly ammoniacal solution. After washing, the oxide was dissolved in saturated oxalic acid, then reprecipitated from 8 N nitric acid containing potassium bromate. After washing, the precipitate was ignited and weighed as Nb_2O_5.

Molybdenum.-- The uranium target was dissolved in hydrochloric acid and the solution completed by the addition of minimum amounts of nitric acid. The solution was boiled to reduce the amount of nitrate and bring the concentration of hydrochloric acid to about 6 N. Molybdenum was extracted with several portions of ether. (A minimum amount of Br_2 was added to the aqueous phase to ensure that molybdenum was present in the VI oxidation state.) The ether layers were combined, washed with 6 N hydrochloric acid, and evaporated over water. Ferric ion and niobium oxalate complex were added to the solution, and their hydrated oxides precipitated by addition of ammonia. The supernatant (containing molybdenum as molybdate) was acidified to about 0.5 N in hydrochloric acid. Molybdenum alpha-benzoin oxime was precipitated from the chilled solution. After washing with 0.5 N sulfuric acid, the oxime was dissolved in concentrated nitric acid and destroyed by boiling carefully to fuming with perchloric acid. After the solution had been cooled and diluted, ferric hydroxide was precipitated using sodium hydroxide. The supernatant was acidified and molybdenum alpha-benzoin oxime reprecipitated and destroyed. After another precipitation of ferric hydroxide, the supernatant was made just acid and buffered with sodium acetate. Molybdenum was precipitated as silver molybdate,

washed, dried at 110°C and weighed as Ag_2MoO_4.

Ruthenium.-- Ruthenium and osmium carriers were added to the nitric acid solution of the target which was then boiled to remove osmium tetroxide. Iodide carrier was added and oxidized with bismuthate to prevent distillation of iodine. Molybdenum was added and complexed with phosphate to prevent distillation of molybdenum. Ruthenium tetroxide was then distilled from fuming perchloric acid in an air stream. To the distillate, trapped in 6 N sodium hydroxide, ethanol was added and the solution boiled to coagulate ruthenium oxide. This may be reoxidized to the higher state and distilled from perchloric acid again for additional purification. The oxide recovered from the alcoholic sodium hydroxide was dissolved in hot 6 N hydrochloric acid. The solution was diluted and the ruthenium reduced to the metallic state with magnesium. The ruthenium was washed, dried at 110°C and weighed as the metal.

Palladium.-- The target solution containing palladium carrier was made about 0.4 N in nitric or hydrochloric acid. Inactive nickel was added as a "holdback" carrier. The palladium was precipitated with dimethylglyoxime and the precipitate washed with dilute acid (0.2 N). The palladium dimethylglyoxime was dissolved in concentrated nitric acid (destroying the dimethylglyoxime), the solution diluted, and ferric hydroxide precipitated twice with ammonia. Silver iodide was precipitated twice (using excess iodide) and the solution reacidified to 0.4 N in hydrochloric acid. After centrifuging out any silver chloride which might have been present, the palladium was precipitated with dimethylglyoxime. The procedure could be repeated for additional purification. After washing, the final palladium dimethylglyoxime precipitate was dried at 110°C and weighed as Pd-dmg.

Silver.-- The target was dissolved in nitric acid containing silver carrier (to avoid adsorption of trace amounts of silver by the glass). The solution was diluted to approximately 4 N in nitric acid and silver chloride precipitated from a boiling solution with stirring. Coagulation is rapid and complete under these conditions. The silver chloride was dissolved in aqueous ammonia and ferric hydroxide was precipitated to remove ammonium hydroxide group contaminants. The silver was recovered by precipitation as silver sulfide. The sulfide was dissolved in concentrated nitric acid which was boiled, then diluted to approximately 4 N for precipitation of silver chloride. The cycle was repeated for additional purification. After dissolving the final precipitate of silver sulfide, the solution was diluted and made basic with ammonia. Ferric hydroxide was precipitated to remove any sulfur which might have been present. The supernatant was made approximately 4 N in nitric acid and silver chloride precipitated. After washing and drying at 110°C, silver was determined as silver chloride. All silver chloride precipitations except the final one should be made in the presence of palladium and cadmium "holdback" carriers to minimize occlusion of radioactive contaminants on the surface of the silver chloride.

Cadmium.-- The target solution containing cadmium carrier and copper was made basic with ammonia. Cadmium and copper were leached out of the massive precipitate by hot aqueous ammonia. The completeness of the extraction was indicated by the cupri-ammonium complex. Iron, lanthanum, and indium were precipitated from the ammoniacal solution. Cadmium and copper sulfides, precipitated from the supernatant, were dissolved in concentrated nitric acid. The solution was diluted to approximately 4 N and silver chloride precipitated. The supernatant was neutralized with ammonia; enough solid potassium cyanide added to complex copper; and cadmium

sulfide precipitated with hydrogen sulfide. The cadmium sulfide was dissolved in 6 N hydrochloric acid, the solution diluted to 2 N, and palladium sulfide precipitated from the hot solution. Antimony sulfide was precipitated from the supernatant. After centrifugation and decantation, the supernatant was made basic with ammonia and cadmium sulfide precipitated. The precipitate was washed, dried at 110°C, and cadmium determined as CdS.

Tin.-- The target was dissolved in hydrochloric acid containing tin carrier. A minimum amount of nitric acid was used to complete the solution of the uranium. A portion of the target solution was taken and diluted to approximately 1 N in acid. Stannic sulfide was precipitated from the hot solution. After washing, the sulfide was dissolved in concentrated hydrochloric acid and the hydrogen sulfide boiled out. The solution was diluted to 2-2.5 N, and antimony sulfide precipitated from the hot solution. The acidity of the supernatant was reduced by the addition of ammonium hydroxide, and stannic sulfide again precipitated. After dissolving the sulfide in hydrochloric acid and boiling out hydrogen sulfide, the solution was diluted and ruthenium, zirconium, niobium, cadmium and iron carriers added. The solution was made basic with excess 6 N sodium hydroxide. Iron was added to the supernatant and the hydroxide again precipitated. The supernatant was acidified and tin precipitated with hydrogen sulfide. The sulfide was dissolved in hydrochloric acid and antimony sulfide reprecipitated. After the tin sulfide was recovered from the supernatant, it was dissolved in nitric acid and metastannic acid precipitated by the addition of solid ammonium nitrate. The precipitate was filtered, ignited, and weighed as SnO_2.

A modification to this procedure has been suggested by Douthett.[8] The antimony was removed by reduction to metallic antimony with iron.

The solution was filtered through "fine" grade sintered glass funnels. Tin was recovered by precipitation of the sulfide from the filtrate. In the sodium hydroxide precipitation of possible contaminants, ammonium polysulfide was added to remove certain elements, such as lead, which would otherwise be soluble in the basic solution. The final precipitate of stannic sulfide was dissolved in ammonium nitrate solution with small amounts of 6 N nitric acid (instead of in concentrated nitric acid) to minimize the amount of sulfur formed.

Tellurium.-- The target was dissolved in hydrochloric acid containing tellurium carrier with the minimum amount of nitric acid necessary to complete solution. A portion of the target solution, to which selenium carrier had been added, was boiled to near dryness with concentrated hydrobromic acid two or three times. The residue was taken up in concentrated hydrochloric acid, selenium carrier added, and the red allotropic modification of selenium precipitated by the addition of sulfur dioxide to the solution at 5°C. The supernatant was diluted to approximately 3 N in hydrochloric acid and tellurium was precipitated by the addition of sulfur dioxide. The tellurium was dissolved in a few drops of concentrated nitric acid, the excess nitric acid evaporated, and the solution diluted. 6 N sodium hydroxide was added dropwise until the precipitate of tellurous acid which formed was thoroughly dissolved. Ferric hydroxide was precipitated from this solution. Tellurium was recovered by precipitation with sulfur dioxide from the acidified supernatant. The procedure was repeated for additional purification. The final tellurium precipitate was washed, dried at 110°C, and weighed as Te.

Cesium.-- (See rubidium procedure, page 27.) The cesium and rubidium perchlorates were taken up in 6 N hydrochloric acid and cesium precipitated

with silicowolframic acid. After digestion at 95°C, the solution was chilled and centrifuged. The precipitate was washed with 6 N hydrochloric acid and dissolved in dilute sodium hydroxide. Upon reacidification, wolframic oxide and silica precipitated. Inert rubidium was added as "holdback" carrier, and the cesium reprecipitated with silicowolframic acid. The precipitate was dissolved and cesium reprecipitated as before. The precipitate was washed with 6 N hydrochloric acid, dried at 110°C and the cesium determined as $Cs_8SiW_{12}O_{42}$.

Barium.-- (See strontium procedure, page 27.) The barium chromate separated from the strontium was washed with water at 95°C. The precipitate was dissolved in a minimum amount of hot 6 N hydrochloric acid. The solution was taken up in ether-concentrated hydrochloric acid, 1:5 by volume, the "ether-HCl reagent." Upon chilling at ice temperature, the barium chloride precipitated. The chloride was dissolved in a minimum amount of distilled water and reprecipitated twice. The final precipitate was washed with absolute alcohol and with ether, and dried in a vacuum dessicator. The barium was determined as $BaCl_2 \cdot 2H_2O$.

Identification of Radioactive Nuclides

Strontium.-- From decay measurements a 9.7 hour strontium activity was observed. A 60 day yttrium activity was chemically separated from the strontium sample, indicating the presence of Sr^{91}. Another strontium sample, from which yttrium had been removed a week after bombardment of the target, showed an activity of 54 day half-life. This was thought to be Sr^{89}.

Aluminum absorption measurements on the 54 day activity showed the characteristic 1.5 mev beta particle of Sr^{89}. The electromagnetic

background was negligible.

Zirconium.-- The zirconium decay showed a 17 hour activity which grew a 69 minute daughter. After decay of the 17 hour Zr^{97}, a decay line of predominantly 65 day half-life was seen.

Niobium.-- Four major species were identified in the niobium decay: 68 minute Nb^{97}; an activity of approximately 23 hours, probably Nb^{96}; 90 hour Nb^{95m} obtained by analytical treatment of the counting data (see page 16); and 37 day Nb^{95}.

Molybdenum.-- The only activity observed in the molybdenum fraction was the 67 hour Mo^{99}.

Ruthenium.-- Decay measurements showed a 4.4 hour activity and longer components. After allowing one year for intermediate activities to die out, decay for a period of eight to nine months showed a one year activity. When the activity due to this component was subtracted from the earlier data, an activity of approximately 43 day half-life was observed. Subtraction of this in turn showed a 37 hour activity, indicating the presence of 4.4 hour Ru^{105} decaying to 37 hour Rh^{105}. The 43 day activity was presumed to be Ru^{103}.

Aluminum absorption measurements on the one year activity showed the characteristic hard beta particles of the Rh^{106} daughter in equilibrium with 1.0 year Ru^{106}.

Palladium.-- Two palladium activities were observed directly, 21 hour Pd^{112} and 14 hour Pd^{109}. The formation of 26 minute Pd^{111} was demonstrated by the separation of 7.5 day Ag^{111} from a portion of the target immediately after bombardment and from a second portion after an interval of three to four hours. The specific activity of Ag^{111} was significantly higher in the second portion than in the first, indicating its formation by the decay

of Pd^{111}.

Decay was measured without absorber, through 80 mg/cm^2 of aluminum (to block the beta particles of Pd^{112}), and through 490 mg/cm^2 of aluminum (blocking the beta particles of Pd^{112} and Pd^{109}, but allowing the radiation of 3.2 hour Ag^{112} in equilibrium to be counted). Growth of the 3.2 hour Ag^{112} was observed.

Silver.-- Decay through 1380 mg/cm^2 Al (to block all particulate radiation from silver isotopes except that of Ag^{112}) showed the 3.2 hour Ag^{112}. Decay without absorber on a sample separated very soon after bombardment (to minimize growth of 3.2 hour Ag^{112} from 21 hour Pd^{112}) emphasized the 5.3 hour Ag^{113}. The 7.5 day Ag^{111} was clearly seen, and shown to be formed (see above) as a primary fission product, its independent yield being 18-20 percent of the total observed β^- chain. Decay followed over a period of ten months showed an activity of 250-270 days, presumably Ag^{110}.

The formation of 20 minute Ag^{115} was shown by separating 53 hour Cd^{115} from a portion of the target immediately after bombardment and from a second portion after an interval of about four hours. The specific activity of Cd^{115} separated from the second portion was significantly higher than that from the first portion, indicating its formation by decay of Ag^{115}.

A sample of silver was initially separated from cadmium, then allowed to decay. Cadmium separated from this sample after four hours showed a 53 hour decay half-life with no indication of a 43 day component. This indicates that Ag^{115} decays predominantly to Cd^{115} ground state rather than to Cd^{115m}.

Aluminum absorption measurements on the 3.2 hour activity showed the characteristic 3.6 mev beta particle of Ag^{112}. Measurements on the 7.5 day activity showed the 1 mev beta energy of Ag^{111}. The electromagnetic

background was less than 0.05 percent of the initial activity. Correcting for the difference in counting efficiencies, this means that any 8.6 day Ag^{106} must be present to less than 5 percent of the Ag^{111}.

Cadmium.-- Decay through 946 mg/cm^2 of beryllium (to block all particles of energy less than 1.9 mev) showed evidence of the 49 minute Cd^{111m} and indicated the possible presence of 6.7 hour Cd^{107}. Decay of the beta radiation showed 2.8 hour Cd^{117}, 53 hour Cd^{115}, and 43 day Cd^{115m}. There was a very long lived component which suggested the presence of 470 day Cd^{109}. Aluminum absorption measurements showed the 1.1 mev beta particle of the 53 hour Cd^{115}.

Tin.-- Decay measurements showed components of about 27 hour, 9.5 day, and a longer component, presumably 130 day. These seem to be Sn^{121}, Sn^{125}, and Sn^{123}, respectively. The other isomer of each mass was not observed.

Tellurium.-- Of the many components in the tellurium decay curve, it was possible to resolve out only the 30 hour Te^{131m} and its 8 day I^{131} granddaughter.

Cesium.-- The predominant activity in the cesium fraction was the 13 day Cs^{136}. Aluminum absorption measurements of this activity showed the characteristic 0.3 mev beta energy of Cs^{136}. Comparison of the activity observed through aluminum absorbers and through beryllium absorbers indicated soft electromagnetic radiation (of the order of K x-rays in this region) present to the extent of about 15 percent of the particulate radiation. This indicates relatively good yields of neutron deficient cesium isotopes decaying by orbital electron capture.

Barium.-- Most of the bombardments were interrelated by measuring the amount of 12.8 day Ba^{140} produced, and using this as an internal monitor. In most cases the barium was not separated from radium. In these cases,

the sample was counted through enough aluminum absorber to prevent any alpha particles emitted by radium or its daughters from reaching the counter tube. In addition to observing its half-life, Ba^{140} was identified by observing the growth of its 40 hour La^{140} daughter.

A sample of barium was analyzed in the mass spectrograph.* The emulsion side of the collector plate was placed against the emulsion of a second plate and the radioactive species allowed to decay for a period of about two weeks. Lines on the second or "transfer" plate indicated radioactive barium isotopes of masses 131, 133, 135, and 140 in comparable yields. An approximately 10 day activity was observed in a cesium sample separated from a purified barium sample some time after bombardment.

Although Ba^{131} has approximately the same half-life and may be present in yields of the same order of magnitude as Ba^{140}, the Geiger activity of $Ba\text{-}Cs^{131}$ contributes less than 1 percent to the Geiger activity of $Ba\text{-}La^{140}$ because of the large difference in counting efficiencies.

Components of 29 to 39 hours having soft particle radiation were observed in the decay curves. An 85 minute component, presumably Ba^{139}, was also observed. In a sample of barium separated from radium on an ion-exchange column, the 85 minute, 29 to 39 hour, and 12.8 day components were observed. The positrons of Ba^{129} were not observed on a crude beta ray spectrometer measurement of the column separated barium.

D. Rare Earth Nuclides: Z = 57 to Z = 71

Chemical Procedure**

General.-- One milligram of each rare earth to be isolated (except promethium, for which tracer was added) was added as carrier, the total

---

*Mass spectrographic analysis by F. L. Reynolds.

**Modification of a procedure used by Wilkinson and Hicks.[27]

amount being of the order of twelve milligrams. The group was separated by precipitation of the fluorides from 2 N nitric acid solution by addition of hydrofluoric acid. (Some uranium fluoride may carry if the concentration of uranium is high enough. For one of the bombardments which used an eight gram uranium target, the uranium was extracted with ether from the nitric acid solution before the rare earth fluorides were precipitated.) The fluorides were dissolved in 8 N nitric acid saturated with boric acid, and the rare earths were recovered as hydroxides by precipitation with ammonia gas. The hydroxides were washed to remove excess ammonium salts, and dissolved in dilute hydrochloric acid. Selected sulfides (copper, arsenic, antimony, tin, silver, palladium, bismuth) were precipitated from this solution by addition of H_2S gas to remove contaminants belonging to the acid sulfide group. From a hydrochloric acid concentration of the order 0.3 N, the rare earths were then precipitated as oxalates. After washing, the oxalates were dissolved in concentrated nitric acid containing potassium bromate. The solution was diluted and the rare earth hydroxides reprecipitated. The hydroxides were dissolved in 0.2 N hydrochloric acid which was then diluted to between pH 1 and pH 2. The solution was equilibrated with Dowex-50 ion exchange resin for five minutes at 95°C.

Cerium.-- In addition to separation by the general procedure, cerium has also been separated from the other rare earths by oxidation to cerium(IV) and precipitation of ceric iodate. Ceric phosphate precipitations have also been used to separate cerium from the other rare earths.

Europium.-- Europium was separated from the other rare earths by reduction to europium(II) with zinc amalgam in a nitrogen atmosphere. The other rare earths were precipitated as hydroxides from a carbonate free solution leaving the europium(II) in solution. The europium was recovered

by ozone oxidation to europium(III) and hydroxide or oxalate precipitation. The cycle may be repeated for additional purification.

Column Separations

The resin, with adsorbed rare earths, was placed in a band at the top of a glass column 4 mm in diameter and 10 cm high, previously packed with resin, and eluted with constant boiling (~6 N) hydrochloric acid at a temperature of 87°C, using a flow rate of approximately 0.1 ml per minute. After about two hours, the rare earths from lutetium through neodymium had been eluted, leaving behind about 30 percent of the praseodymium, 50 percent of the cerium, 60 percent of the lanthanum and all of the actinium with its thorium daughter activities.

The rare earths were recovered from the 6 N hydrochloric acid solution by precipitation of the hydroxides with ammonia gas. The hydroxides were washed, dissolved, and equilibrated with resin as before. The resin was then placed at the top of a glass column 7 mm in diameter and 20 cm high, previously packed with resin, and eluted with 0.25 M ammonium citrate-citric acid solutions at 87°C. Lutetium and ytterbium were separated by elution with pH 3.19 citrate at a flow rate of 0.14 ml per minute. Ytterbium, thulium, erbium, and holmium were separated by elution with pH 3.23 citrate at a flow rate of 0.21 ml per minute. For the lighter rare earths, pH 3.30 and pH 3.5 citrate solutions were used successively. Dysprosium-yttrium and europium-gadolinium were not separated under these conditions. The dysprosium-yttrium separation was made by elution with pH 3.05 citrate on another resin-packed column at room temperature.

Recovery and Chemical Yield

By means of a turntable actuated by a microflex timer, samples of the elutriant were collected at regular intervals. Small aliquots of these samples were mounted on counting plates for radioassay. From the plot of relative activity versus sample number it was possible to identify the various peaks representing the separated rare earths. Identification of the peaks was made more definite by spectrographic analysis.

From the radioassay plot it was possible to select the samples comprising a given peak which were free from any contamination by neighboring peaks. These samples were combined in a small erlenmeyer flask and fumed with sulfuric acid to which a few drops of selenium(IV) solution were added as a catalyst. The destruction of the citrate was completed by adding perchloric acid and heating. The rare earth was recovered by precipitation as the hydroxide. After washing out the ammonium perchlorate, the hydroxide was dissolved and the oxalate precipitated. The oxalate was dried in a vacuum dessicator at room temperature, and weighed to determine the percentage recovery of the rare earth. (The oxalate was selected for the gravimetric analysis because of its high molecular weight. In this way small amounts of a rare earth could be determined with greater accuracy since there are four to five grams of the compound per gram of rare earth.)

Identification of Radioactive Nuclides

Lanthanum.-- Decay curves showed essentially a single component, the 40 hour La^{140}, over a period of 8-9 half-lives. Decay of the radiation passed through 946 mg/cm^2 of beryllium (to block the particles and give other electromagnetic radiation a more favorable counting efficiency relative to La^{140}) gave a curve essentially parallel to the curve taken without absorber. Since the final separation of lanthanum was not

accomplished until 56 hours after bombardment, the possibility of formation of nuclides of shorter half-life in comparable yield is not excluded.

Aluminum.-- Absorption curves of the 40 hour activity compared closely with absorption curves of the radiations from the 40 hour β^- daughter of Ba^{140}. From the absorption curves the counting rate was corrected for air and window absorption, and for the contribution of the electromagnetic radiation. The disintegration rate was calculated from this corrected counting rate.

Calculations based on the relative yields of Ba^{140}, La^{140}, and Nd^{140} (explained in the following section) show that ~30 percent of the total mass 140 yield is formed as La^{140}.

Cerium.-- Decay curves showed components of approximately 35 hour component and approximately 30 day with a component of intermediate half-life. Analysis of the data indicated Ce^{143} with Pr^{143} daughter, and Ce^{141}. Decay over a period of about six months indicated the presence of 275 day Ce^{144}.

Comparison of the number of x-rays emitted by the long lived activity with the number from Ce^{144} tracer obtained from slow neutron fission of uranium indicated the presence of 140 day Ce^{139} in our sample. Aluminum absorption measurements on the long lived component showed two beta components which could be attributed to Ce^{144} and the 17 minute Pr^{144} in equilibrium.

Praseodymium.-- Decay through 406 mg/cm^2 of aluminum showed a 19 hour half-life. Decay without absorber showed two components, one of 13.5 day half-life, the second (by subtraction) of half-life 16 to 19 hours. Aluminum absorption measurements on the 19 hour activity showed hard beta radiation of 2.3 mev energy and indicated a soft component of about 0.6 mev

energy in about 20 percent abundance. After decay of the 19 hour activity, aluminum absorption measurements of the 13.5 day activity showed a particle of 0.92 mev maximum energy. On the basis of the decay and absorption measurements, it was concluded that Pr^{142} and Pr^{143} were both present in good yield.

Pr^{142} is a shielded nuclide; consequently, its independent yield was obtained directly. The independent yield of Pr^{143} was obtained by removal of the 33 hour Ce^{143} parent from the rare earth group within two hours after bombardment. Since the ratio of the yield of Pr^{143} to that of Pr^{142} was about 1.7, the Pr^{143} represents a greater fraction of the total mass 143 chain than the Pr^{142} does of its chain. This indicates that whereas the most probable primary charge for a given mass had been on the neutron excess side, the trend is for the most probable primary product to be much closer to stability for the higher mass chains.

Neodymium.-- Decay through 407 mg/cm^2 of beryllium (sufficient to block the beta particles of Nd^{147}) showed two components. After subtraction of the 11 day tail due to the gamma ray of Nd^{147}, a 3.3 day line was found. This is the activity assigned to Nd^{140} by Wilkinson and Hicks.[28] Decay without absorber showed the 11 day line of Nd^{147} for over three half-lives. Aluminum absorption curves showed the characteristic beta particle energy of Nd^{147}. Since less than 2 percent of the initial total activity could be attributed to Nd^{140}, this activity did not interfere and was not characterized by absorption. Its counting efficiency was calculated from the data of Wilkinson and Hicks.[28]

Calculations based on the relative yields of Ba^{140}, La^{140}, and Nd^{140} show that ~7.5 percent of the total mass 140 yield is formed as Nd^{140}.

Promethium.-- Decay was followed both without absorber and through 485 mg/cm^2 of aluminum (sufficient to block the beta particles of Pm^{149}). The decay without absorber showed components of approximately 13 hours, of 47 hours, and of about 43 days. Decay of the radiations passed through the absorber showed components of 47 hours (the gamma ray of Pm^{149}), 5.3 days, and 43 days. Of the activities, only the 47 hour Pm^{149} and the 5.3 day Pm^{148} have been assigned. A 12.5 hour promethium activity has previously been reported, but no mass assignment was given. The 43 day activity represents a previously unreported nuclide.

Absorption of the radiations of the 47 hour activity showed a single beta component of about 1.1 mev energy. This is the reported maximum energy for the beta particles of Pm^{149}. After decay of the 47 hour and 5.3 day components, absorption measurements of the 43 day activity were made. Aluminum absorption showed two beta components of energies ~0.5 mev and ~2.3 mev. The hard component was present to only 5 to 10 percent abundance. The sample was also measured on a crude beta ray spectrometer which showed (from a Fermi-Kurie plot of the data) β^- components of 0.6 and 2.4 mev. The electromagnetic background of the aluminum absorption curve was of the order of 3 percent. After blocking the particulate radiation with beryllium absorber, the electromagnetic component was absorbed in copper. No K x-rays of neodymium (which have a half-thickness of 165 mg/cm^2 in copper) were observed. Absorption of the electromagnetic radiation in lead showed a half-thickness of 7.3 g/cm^2 which corresponds to a gamma ray of approximately 0.9 mev energy.

The yield of the shielded Pm^{148} is only about 1 percent of that for the Pm^{149} which represents the total β^- chain for its mass. The yield of the 43 day promethium is about 10 percent of that for Pm^{149}. On the

basis of yield and the fact that this activity was not reported formed in slow neutron fission or by Nd(n,γ) reaction, a tentative assignment of the 43 day activity to Pm^{150} is made.

Samarium.— The samarium decay showed components of about 10 hours and of 47 hours, the 47 hour component being quite prominent. After decay of this activity, a 15-16 day line was observed. Aluminum absorption measurements of the 47 hour activity indicated a beta particle of about 0.8 mev energy. In the absorption measurements the 2.4 mev β^- of Eu^{156} was also observed.

The principal activities found in the samarium fraction were the 47 hour Sm^{153} and the 10 hour Sm^{156} with its 15.4 day Eu^{156} daughter. The yield of Sm^{156} relative to Sm^{153} was only 27 percent. The yield of Sm^{153} represents the entire β^- chain for mass 153 whereas Eu^{156} is expected to be a large contributor to the mass 156 yield.

Europium.— The principal europium activity seen was the 15.4 day Eu^{156}. Aluminum absorption showed the characteristic 2.4 mev β^- of Eu^{156}.

Terbium.— The terbium decay curve resolved roughly into two components, the longer of which had a half-life of 74 days. The shorter component was a mixture of activities between 5 and 7 days with a yet shorter portion. Decay was observed without absorber and also through 183 mg/cm^2 of beryllium (sufficient to block the 0.5 mev β^- particles of Tb^{161}). After subtraction of the 74 day residium, the decay through beryllium showed strong indication of a 5.1 day activity. The decay without absorber showed a mixed activity with the 6.8 day activity predominating after subtraction of the 74 day component.

In the terbium fractions separated 12 to 14 hours after bombardment, traces of alpha activity were observed. A sample submitted to Mr. J. O.

Rasmussen for alpha pulse analysis showed alpha energy and decay corresponding to 4.5 hour Tb^{149}.

Dysprosium.— The chief component observed in the dysprosium decay was the 80 hour Dy^{166}. A long lived activity was also observed, but we were unable to determine its half-life. Aluminum absorption measurements on the equilibrium mixture showed the 0.4 mev beta particle of Dy^{166} and the ~1.9 mev beta particle of the Ho^{166} daughter.

Calculations based on the relative yields of Dy^{166}, Ho^{166}, and Yb^{166} indicate that 2.54 percent of the total mass 166 yield is formed as Dy^{166}.

Holmium.-- The major component observed in the holmium decay was the 27 hour Ho^{166}. The decay was followed through eight half-lives. Less than 0.02 percent of the Ho^{166} activity present at end of bombardment remained as long lived component. Aluminum absorption measurements showed the ~1.9 mev beta energy of Ho^{166}.

Calculations based on the relative yields of Dy^{166}, Ho^{166}, and Yb^{166} indicate that 4.7 percent of the total mass 166 yield is formed as Ho^{166}.

Erbium.-- The erbium sample first showed growth which was identified as a holmium activity from the radioassay plot. The erbium peak showed growth while the trough between the erbium and holmium showed rapid decay. This indicated a new erbium activity decaying by orbital electron capture and/or positron emission to a short lived holmium activity. Decay was observed without absorber and also through 99.7 mg/cm^2 of beryllium (to block the beta particles of Er^{169}). Two new activities were observed in the decay through absorber; one of about 17 hour half-life and the other of 65 hour half-life. The decay without absorber showed a mixture of these activities and a component of 9.4 day, the Er^{169}.

The growth observed had a 4.5 hour half-life. The holmium activity[29] of this half-life is assigned to Ho^{161}. The 7 day activity presently assigned to Ho^{163} was not observed in our holmium sample in a resolvable amount. This may indicate that the 7 day holmium is shielded, hence Ho^{162}.

Thulium.-- Decay without absorber showed an approximately 10 day activity prominently. Decay through ~40 mg/cm^2 of aluminum and decay through ~60 mg/cm^2 of beryllium emphasized an activity of two to three days half-life. These absorbers blocked the conversion electrons of 9.6 day Tm. The 9.6 day was masked to such an extent by the absorbers that it was not resolvable graphically from the shorter activity. Since an activity on the neutron deficient side of stability in this region would be expected to have about the same counting efficiency as the 9.6 day Tm^-, it is felt that the two to three day activity represents a negative beta transition.

Ytterbium.-- The ytterbium decay curve showed components of 32 days and 62 hours. The sample showed growth of a 7.7 hour activity which was shown to be thulium by observing the growth and decay of the radioassay samples (i.e., growth of the ytterbium peak and decay of the trough between the ytterbium and thulium peaks). From an estimate of the time of separation from thulium, the counting efficiency of the ytterbium parent was found to be small compared to the thulium daughter.* On the basis of the assignment of the 7.7 hour thulium activity[27] to Tm^{166}, the new 62 hour ytterbium activity is assigned to Yb^{166}.

Aluminum absorption measurements on the 62 hour activity showed the presence of conversion electrons, a hard beta particle, and electromagnetic radiation background. The relative abundance of electrons and hard beta particles (2 mev) compared with those reported for the particles[27] from

---

*Appendix I.

Tm^{166}. Beryllium and copper-beryllium measurements of the 32 day activity showed electrons, x-rays, and gamma rays comparable to some of those reported for 32.5 day Yb^{169}. 99 hour Yb^{175} was not detected either by decay or absorption.

Isobaric chain yield calculations indicated that 13.5 percent of the total yield of mass 166 was formed as Yb^{166}. The most probable primary charge for the nuclide of this mass is Z = 71.

E. Tabulation of Observed Yields

Formation cross sections were measured for the following nuclides including their precursors (i.e., total β^- chains):

Table I

Nuclide	σ_f (mb.)	Y_R (Ba^{140} = 1.00)
Cu^{67}	2.1	0.09
Se^{81m}	7.5	0.32
Sr^{89}	35	1.5
Ag^{111}	48.5	2.1
Cd^{115}	33.6	1.4
Cd^{115m}	12	0.51
Ba^{140}	23.5	1.0

By means of these, the relative yield values, Y_R, (Ba^{140} taken to be 1.00) given below may be converted to formation cross section values. Integration of the yield versus mass curve (Fig. 1) in terms of the formation cross sections indicates a total fission cross section of 2.0 barns for uranium with 340 to 350 mev protons.

Table II

Mass Number	Nuclide Measured	Y_R	σ (mb)
59	Fe^{59}	0.023	0.54
66	Ni^{66}	0.039	0.92
67	Cu^{67}	0.09	
72	Zn^{72}	0.098	
76	As^{76}	0.0070	
80	Br^{80m}	0.077	
81	Se^{81m}	0.32	
82	Br^{82}	0.064	
83	Se^{83}	0.025	
	Br^{83}	0.28	
84	Br^{84}	0.098	
86	Rb^{86}	0.60	
89	Sr^{89}	1.5	
91	Sr^{91}	1.5	
106	Ru^{106}	2.5	
111	Pd^{111}	1.6_5	
	Ag^{111}	0.4_1	
115	Cd^{115}	1.4_3	
	Cd^{115m}	0.51	
117	Cd^{117}		
131	Te^{131m}	0.25	
136	Cs^{136}	0.25	
139	Ba^{139}	1.80	

Table II (Cont.)

Mass Number	Nuclide Measured	Y_R
140	Ba^{140}	1.00
	La^{140}	0.48
	Nd^{140}	0.18
142	Pr^{142}	0.33
143	Pr^{143}	0.55
147	Nd^{147}	1.4
153	Sm^{153}	0.19
156	Sm^{156}	0.05
	Eu^{156}	0.12
166	Dy^{166}	0.0019
	Ho^{166}	0.0020
	Yb^{166}	0.030
193	Os^{193}	0.00043
~198	$Au^{198,199}$	0.00094
224	Ra^{224}	0.12
236	(p,3n) reaction*	0.51

*W. W. Meinke, G. C. Wick, and G. T. Seaborg, University of California Radiation Laboratory Report UCRL-868 (September 26, 1950).

III. ISOBARIC YIELD STUDIES

A. Introduction

As mentioned in the introduction (cf., page 6) identification of the charge of the fissioning nucleus depends upon the determination of the primary fission products. Experimentally we have attempted to measure the independent yields of various members of several reference mass chains. The nuclide whose yield is the maximum of the curve obtained by plotting the independent yield as a function of atomic number for a given mass is defined to be the primary product for that mass. In practice it is usually quite difficult experimentally to measure directly the independent yields for all of the members of a given mass chain. Those independent yields which have been measured experimentally are listed in Table III below. The yields of the measured members furthest from stability for any chain included the yields of their precursors.

B. Experimental Techniques

Of the several techniques used in measuring independent yields, the choice depends upon the half-lives and the relative difficulty of the separation chemistry for the species sought. Example I (Mass 111):

$$Pd^{111} \xrightarrow[26\ min]{\beta^-} Ag^{111} \xrightarrow[7.5\ day]{\beta^-}$$

The uranyl nitrate target was bombarded for 2.0 minutes, fused, poured into a dissolver solution containing a known quantity of silver carrier and some palladium "holdback" carrier, and the solution divided. From one portion, silver chloride was immediately precipitated to separate from palladium. This separation was accomplished within three minutes after the end of the bombardment. The other portion was allowed to stand until the 26 minute Pd^{111} had all decayed to Ag^{111}. The silver fractions were then

Table III

Mass Number	Nuclide Measured	Relative Yield	Estimated Fraction of Total Chain
83	Se^{83}	0.025	0.05
	Br^{83}	0.28	0.6
86	Rb^{86}	0.60	0.6
111	Pd^{111}	1.6_5	0.5
	Ag^{111}	0.4_1	0.08
140	Ba^{140}	1.00	0.43
	La^{140}	0.48	0.21
	Nd^{140}	0.18	0.075
166	Dy^{166}	0.0019	0.044
	Ho^{166}	0.0020	0.047
	Yb^{166}	0.030	0.72

separated and purified. From the initial specific activity of the silver obtained in the two cases and the known half-lives of the two species, it was possible to calculate the independent yield of Ag^{111} and the yield of Pd^{111} plus its precursors. Details of the analytical treatment of the data are discussed below. Example II (Mass 140):

$$Ba^{140} \xrightarrow[12.8\ day]{\beta^-} La^{140} \xrightarrow[40\ hour]{\beta^-}$$

Since the activities involved are relatively long, a one hour bombardment could be used. Separation of the two species was accomplished within one to two hours after bombardment. After purification of the two fractions (cf., page 38) and counting of the radioactive samples, the observed yield of Ba^{140} was used to correct the La^{140} activity for that portion which had grown from barium during bombardment and before separation of the species. In this way the independent yield of La^{140} was obtained.

In cases where the independent yield of daughter activity is small relative to the parent, precautions must be taken to minimize the amount of contribution from the parent in the initially separated sample of daughter activity. This may be done by reducing the bombardment time, minimizing the time elapsed from end of bombardment to initial separation of desired activity, and developing a specific separation procedure which is rapid and essentially complete in one operation.

Independent yields of "shielded" nuclides may be measured directly since the activity could not grow from the neighboring isobars which are stable.

C. Treatment of the Data

When two species are formed independently by bombardment, and one of the species is also formed by decay of the other, the differential equations of formation during the bombardment are (assuming that species 2 is formed by decay of species 1):

$$\frac{dn_1}{dt} = R_1 - \lambda_1 n_1 \qquad \text{(cf., page 8)} \qquad \text{(III-1)}$$

$$\frac{dn_2}{dt} = R_2 + \lambda_1 n_1 - \lambda_2 n_2 \qquad \text{(III-2)}$$

Expressing the number of atoms of species 1 present at the end of a bombardment of duration t as $n_1^{\,o}$ and the number of atoms of species 2 present at this time as $n_2^{\,o}$, integration of Equations (III-1) and (III-2) leads to:

$$n_1^{\,o} = \frac{R_1}{\lambda_1}\left(1-e^{-\lambda_1 t}\right) \qquad \text{(III-3)}$$

$$n_2^{\,o} = \frac{R_2}{\lambda_2}\left(1-e^{-\lambda_2 t}\right) + \frac{R_1}{\lambda_2}\left[\left(1-e^{-\lambda_2 t}\right) + \frac{\lambda_2}{\lambda_1-\lambda_2}\left(e^{-\lambda_1 t} - e^{-\lambda_2 t}\right)\right] \qquad \text{(III-4)}$$

From the integrated decay equations it is possible to relate the number of atoms of each species present at the time of separation, T units after the end of bombardment, to the number of each species present at the end of bombardment.

$$n_1 = n_1^{\,o} e^{-\lambda_1 T} = \frac{R_1}{\lambda_1}\left(1-e^{-\lambda_1 t}\right) e^{-\lambda_1 T} \qquad \text{(III-5)}$$

$$n_2 = n_2^{o} e^{-\lambda_2 T} + \frac{\lambda_1}{\lambda_1 - \lambda_2} n_1^{o} \left(e^{-\lambda_2 T} - e^{-\lambda_1 T}\right)$$

$$= \frac{R_2}{\lambda_2}\left(1-e^{-\lambda_2 T}\right) e^{-\lambda_2 T} + \frac{R_1}{\lambda_2}\left[\left(1-e^{-\lambda_2 t}\right) + \frac{\lambda_2}{\lambda_1-\lambda_2}\left(e^{-\lambda_1 t} - e^{-\lambda_2 t}\right)\right] e^{-\lambda_2 T}$$

$$+ \frac{R_1}{\lambda_1-\lambda_2}\left(1-e^{-\lambda_1 t}\right)\left(e^{-\lambda_2 T} - e^{-\lambda_1 T}\right) \qquad \text{(III-6)}$$

The expression for n_2 may be made more compact as:

$$n_2 = \left(R_2 + \frac{\lambda_1}{\lambda_1-\lambda_2} R_1\right) \frac{\left(1-e^{-\lambda_2 t}\right) e^{-\lambda_2 T}}{\lambda_2} - \frac{R_1}{\lambda_1-\lambda_2}\left(1-e^{-\lambda_1 t}\right) e^{-\lambda_1 T} \qquad \text{(III-7)}$$

When the decay constants of the species sought are of an order such that activities proportional to n_1 and n_2 may be determined directly, R_1 may be determined from Equation (III-5). By substitution of this value into Equation (III-7), R_2 is obtained. This type of calculation was applied to determine the independent rates of formation for Ba^{140} and La^{140}.

When the decay constants of the species sought are such that only the activity of the long lived daughter of a short lived parent may be measured directly, Equations (III-5) and (III-7) may be further manipulated to give expressions for the independent rates of formation of species 1 and 2 in terms of the activities of species 2 measured at two different times of separation. Consider the case for which $\lambda_1 > \lambda_2$ (in the case of Pd^{111} and Ag^{111}, $\lambda_1 \approx 500\ \lambda_2$). A time of separation may be chosen such that $e^{-\lambda_1 T} \approx 0$. Calling the number of atoms of species 2 present at this time, n_∞, extrapolation to the time of end of bombardment gives $n_\infty e^{\lambda_2 T} = n_\infty^{o}$. Call the number of atoms of species 2 present at a time of separation T, soon after the end of the bombardment, n_T. Extrapolation back to the end of bombardment gives n_T^{o}. The independent rates of formation of 1 and 2 are given by:

$$R_1 = \frac{(\lambda_1-\lambda_2)\ (n_\infty{}^o-n_T{}^o)}{(1-e^{-\lambda_1 t})}\ e^{(\lambda_1-\lambda_2)T} \qquad \text{(III-8)}$$

$$R_2 = \frac{\lambda_2 n_\infty{}^o}{(1-e^{-\lambda_2 t})} - \frac{\lambda_1(n_\infty{}^o-n_T{}^o)\ e^{(\lambda_1-\lambda_2)T}}{(1-e^{-\lambda_1 t})} \qquad \text{(III-9)}$$

Since $R = IN\sigma$ (definition, page 8), the ratio of the cross section for independent formation of 2 compared to the total formation cross section of 1 and 2 is given by:

$$\frac{\sigma_2}{\sigma_1+\sigma_2} = 1 - \frac{\lambda_1-\lambda_2}{\lambda_2}\ \frac{(n_\infty{}^o-n_T{}^o)\ (1-e^{-\lambda_2 t})\ e^{(\lambda_1-\lambda_2)T}}{n_\infty{}^o(1-e^{-\lambda_1 t}) - (n_\infty{}^o-n_T{}^o)\ (1-e^{-\lambda_2 t})\ e^{(\lambda_1-\lambda_2)T}} \qquad \text{(III-10)}$$

For $\lambda_1 \gg \lambda_2$

$$\frac{\sigma_2}{\sigma_1+\sigma_2} \simeq 1 - \frac{\lambda_1}{\lambda_2}\ \frac{(n_\infty{}^o-n_T{}^o)\ (1-e^{-\lambda_2 t})\ e^{\lambda_1 T}}{n_\infty{}^o(1-e^{-\lambda_1 t}) - (n_\infty{}^o-n_T{}^o)\ (1-e^{-\lambda_2 t})\ e^{\lambda_1 T}} \qquad \text{(III-11)}$$

The derivation of Equations (III-8) through (III-11) is given in Appendix II. This type of calculation was applied to determine the independent rates of formation for Pd^{111} and Ag^{111}.

D. Interpretation of the Data*

In order to interpret the data obtained for independent yields, we have assumed that the independent yields of the various isobars of a given decay chain are distributed symmetrically about some particular z in a manner which can be well approximated by the normal curve of error, using suitable parameters to adjust the half-width and peak height of such a distribution curve to the experimental results obtained. A description of the

*The following treatment was suggested by Dr. P. C. Stevenson.

mathematical method of fitting the normal curve of error to such data is given in Appendix III.

It will be seen from this Appendix that three experimental data are sufficient to establish the constants of the curve. We can therefore obtain some idea of the validity of our basic assumption by studying the independent yields in chains containing more than three members. Possibly suitable chains are those of masses 166, 141, 111, and 72, each chain containing four measurable members. Initial sets of three experimental data have been obtained for the chains of mass 140 and mass 166. The decay schemes of these chains are shown in Figure 2.

Figures 3 and 4 show the standard-curve-of-error histograms for the mass 140 and mass 166 chains, respectively. It will be seen that the data follow such a curve to within the experimental error in both cases. The parameters for these curves are tabulated in Table IV.

Table IV

	Z_c	Standard Deviation	Z_c/A
mass 140	57	1.9	0.41
mass 166	71	2.7	0.43

It is apparent that if we could predict the parameters of these charge-distribution histograms as functions of the chain mass number, we could derive correction factors for each mass number to give the total chain yield, including stable nuclides, in terms of the yield of any nuclide of the chain. The rough estimates of total chain yields given in Table III were made on the basis of the few data presently available.

IV. SPALLATION PRODUCTS

A. Introduction

The work of O'Connor and Seaborg[4] on the bombardment of uranium with 380 mev helium ions showed that there was apparently a continuous yield of radioactive products for the entire range of elements from the uranium region down to the vicinity of atomic number 25. Above mass 120 the yield of fission products decreased with increasing mass number. In the region above mass 200 the yield curve was observed to increase with increasing mass. This increase was attributed to products formed by high energy spallation of uranium. The yield of products found in the region of the minimum of the curve might be attributed to a combination of fission products and spallation products. That fission can occur in such a manner as to give products of such high mass was shown by the measuring of product nuclei of correspondingly low mass.

In the present work it was observed that the primary fission products tend toward the neutron deficient side of stability with increasing mass number. However, in the region of mass 180 to 200, several β^- emitting nuclides have been observed. These we have attributed tentatively to spallation reactions.

B. Chemical Procedures

Hafnium.-- Hafnium and zirconium were separated together from other fission products by the standard procedure (cf., page 28). Hafnium was separated from zirconium by elution from cation exchange resin with constant boiling hydrochloric acid.[30] Since the hafnium is eluted first, tailing from the higher activity zirconium peak does not interfere.

Osmium.-- After carefully dissolving the uranium target in nitric acid under reflux, carrier osmium having previously been added to the nitric

acid, iodine and bromine "holdback" carriers were added, oxidized with sodium bismuthate, and osmium tetroxide distilled into 6 N sodium hydroxide. Hydrogen sulfide gas was passed in to precipitate osmium sulfide. After washing, the sulfide was dissolved in concentrated nitric acid, and the distillation-precipitation cycle repeated twice. The sulfide precipitate was then dissolved in perchloric acid. Molybdenum "holdback" carrier was added and complexed with phosphate. Osmium tetroxide was distilled from this solution. After precipitation of the sulfide, the perchloric acid distillation was repeated. The solution of osmium in 6 N sodium hydroxide was carefully acidified with hydrochloric acid and the osmium(VIII) reduced with magnesium to metallic osmium.

Gold.-- Gold was separated as the metal by a series of precipitations from chloride-free nitric acid solution with sulfur dioxide in the presence of mercury, tellurium, and platinum "holdback" carriers. The gold was then dissolved in a minimum of aqua regia and taken up in 6 N hydrochloric acid from which it was extracted by ethyl acetate. Gold was recovered by evaporating the organic layer over dilute nitric acid and precipitating metallic gold with sulfur dioxide.

Radium.-- (See barium procedure, page 34.) The final precipitate of barium chloride was washed with alcohol to remove any excess hydrochloric acid. The precipitate was then dissolved in water and equilibrated with cation exchange resin. By elution through a column packed with resin, using pH 8 ammonium citrate solution, the barium and radium fractions were separated.[31] Samples for alpha counting were mounted on platinum disks and flamed to destroy and remove citrate, leaving essentially weightless samples.

C. Results

Hafnium.-- The purified hafnium fraction showed a negative beta activity having an energy of about 0.4 mev and long life. This activity has been attributed to Hf^{181}.

Osmium.-- Decay of the osmium fraction showed a component of about 32 hours half-life which was attributed to Os^{193}.

Gold.-- The decay of the gold sample gave indication of the 14 hour and 5.6 day isomers of Au^{196}. An intermediate activity was observed which seemed to be a mixture of Au^{198} and Au^{199} (2.7 day and 3.3 day, respectively). Aluminum absorption measurement on this activity showed a beta energy of about 1 mev and a softer component whose energy was not determined.

Radium.-- Decay of the radium samples was followed by both Geiger measurements and alpha counting. From the decay curves and pulse analysis of the alpha activity, radium isotopes of mass 223, 224, and 225 were identified. A new Geiger activity, having a half-life of the order one to two hours, was observed in the separated radium fraction. This activity might be from Ra^{227}, Ra^{230}, or a mixture of both.

Actinium.-- The formation of Ac^{226} was indicated by the presence of a short thorium alpha activity eluted from an ion exchange resin column some 20 to 30 hours after bombardment. The activity was identified as thorium by its elution characteristics.

V. DISCUSSION

From examination of the data herein presented, a few marked trends are observed. Almost all of the low mass nuclides identified were of the neutron excess type. As higher mass numbers were approached, neutron deficient nuclides increased in relative abundance of formation. However,

in the spallation region, which merges with the heavy fission fragments in the region of mass 180, neutron-excess nuclides again predominate.

Analysis of the yields of the two beta decay chains so far studied in detail has indicated that the charge to mass ratio of the most probable nuclide formed for a given mass is not a constant independent of the mass. This suggests that consideration should be given to the possibility that the observed fission yield curve is the result, not of a single fissioning species, but of a group of fissioning species whose relative importance is distributed in a manner dependent upon the bombarding energy and the bombarding particle.

Let us consider a nuclide formed by high energy spallation of a U^{238} nucleus, this nuclide having an amount of internal energy much in excess of the fission threshold. This energy may be dissipated in one of three different ways: It may in part be used to cause fission, any excess being carried off by the fission fragments or radiation; it may be dissipated as radiation, the nuclide in question descending to a nonfissioning ground state; or it may be carried off, in part or entirely, by an emitted nucleon or composite particle, such as an alpha particle or a deuteron, leading to a different nuclide which again may undergo one of these three changes. If we represent all the possible nuclides as points on a plane with coordinate axes Z and A-Z, then the various spallation and fission products possible from U^{238} with protons will all fall within the quadrant of this plane having $Z \leq 93$, $A-Z \leq 146$. Normalizing the total probability of fission to unity, the various partial fission probabilities of the nuclei lying within the spallation region can be described by a contour map. The contour lines are the loci of points of equal partial fission probability. The fission fragment yield curve may be plotted in the same way on the same

chart (see Figure 5). The dotted line of slope -1 represents an isobaric chain. The independent yield of the members of this chain as a function of Z is given by the value of the contour line intersected for each Z.

We may assume that the shape of the fissioning-nucleus contour map is markedly energy-sensitive. Let us further assume that the fission-fragment yield distribution is uniquely determined by the fissioning-nucleus distribution. Some qualitative predictions of the behavior of the fission-fragment yield curve with variation of bombarding energy may then be made.

The most obvious effect of increasing the bombardment energy will be to increase the number of spallation products leading to fission, since Douthett[8] has shown that excess bombarding energy does not appear as kinetic energy of the fragments. This will lead to a lower average mass for the "fissioning nucleus," with its concurrent effect of lowering the mass of the maximum yield of fission fragments. Also, should neutrons be evaporated from the excited nuclides in preference to protons or other charged particles, as seems likely, the charge-to-mass ratio of the average fissioning nucleus, and hence of its fragments, should be increased. We thus expect that at high energies nuclides closer to stability, or even on the neutron deficient side, should appear in greater relative abundance, as is actually observed.

In order to confirm these points, it is desired to make a study, at various bombarding energies, of a number of the experimentally available isobaric chains. It is also desired to make an intensive study at full proton energy of the yields on the fission-spallation overlap region. Some evidence exists to show that spallation products are formed mainly by alpha particle evaporation, which would yield neutron-excess products in the overlap region; fission, as we have said, is expected to yield neutron

deficient nuclides in this region. The transition from one type of fragment to the other with increasing mass number should be most informative.

VI. ACKNOWLEDGMENTS

I wish to express my gratitude to Professor Glenn T. Seaborg under whose guidance this work was done, to Professor I. Perlman for continued interest and advice, and to my collaborator Dr. Peter Stevenson for his contributions to experimental technique and theoretical interpretation. I also wish to thank Professor L. Malatesta, Doctors H. Hicks, J. Miller, and B. C. Haldar, and Mssrs. G. Higgins, G. Rudstam, W. Worthington, and W. Nervik for their material assistance in performing experiments and obtaining data for various phases of the work. The cooperation of Mr. J. T. Vale and Mr. Lloyd Hauser and all those of the 184-inch cyclotron group is gratefully acknowledged. I wish to thank Mssrs. J. Conway and M. Moore who provided spectrographic analyses of the uranium target material and of many of the samples, particularly the rare earths, to indicate their purity. I wish to express appreciation to Mrs. Elinor Potter and Mrs. Roberta Garrett for valuable assistance in the counting of samples. This work was performed under the auspices of the Atomic Energy Commission.

APPENDIX I

The counting efficiency of a radioactive nuclide which decays to a second radioactive species may be determined from the growth and decay curve of the equilibrium mixture when the counting efficiency of the second activity is known. Consider the decay

$$X \xrightarrow{\lambda_x} Y \xrightarrow{\lambda_y} Z \text{ (stable)}, \quad \lambda_y > \lambda_x,$$

where λ represents the decay constant. From the classical decay laws, the activities of X and Y, respectively, are given by:

$$\lambda_x X = \lambda_x X^o e^{-\lambda_x t} \tag{AI-1}$$

$$\lambda_y Y = \frac{\lambda_x \lambda_y X^o}{\lambda_y - \lambda_x} \left(e^{-\lambda_x t} - e^{-\lambda_y t}\right) \tag{AI-2}$$

In the equations, X and Y represent the number of atoms of X and Y, respectively. Let k_x represent the counting efficiency of activity X and k_y that of Y. The observed counting rates at a particular geometry are:

$$C_x = g k_x \lambda_x X \tag{AI-3}$$

$$C_y = g k_y \lambda_y Y \tag{AI-4}$$

where g is a factor determined by the geometry. The total observed counting rate, from the preceding equations, is:

$$C = C_x + C_y = g\left[k_x \lambda_x X^o e^{-\lambda_x t} + \frac{k_y \lambda_y \lambda_x X^o}{\lambda_y - \lambda_x} \left(e^{-\lambda_x t} - e^{-\lambda_y t}\right)\right] \tag{AI-5}$$

$$C = g\lambda_x X^o \left[e^{-\lambda_x t} \left(k_x + \frac{\lambda_y}{\lambda_y - \lambda_x} k_y\right) - e^{-\lambda_y t} \frac{\lambda_y}{\lambda_y - \lambda_x} k_y\right] \tag{AI-6}$$

At large t such that $e^{-\lambda_y t} \longrightarrow 0$, we obtain from (AI-6):

$$C' = g\lambda_x X^o \left[k_x + \frac{\lambda_y}{\lambda_y - \lambda_x} k_y \right] e^{-\lambda_x t} \qquad \text{(AI-7)}$$

Subtraction (AI-6) from (AI-7):

$$C' - C = g\lambda_x X^o \left[\frac{\lambda_y}{\lambda_y - \lambda_x} k_y \right] e^{-\lambda_y t} \qquad \text{(AI-8)}$$

At the time of separation, t = o

$$(C'-C)^o = \frac{g\lambda_x X^o k_y \lambda_y}{\lambda_y - \lambda_x} = A \qquad \text{(AI-9)}$$

From (AI-7) and (AI-9):

$$(C')^o = g\lambda_x X^o k_x + \frac{g\lambda_x X^o k_y \lambda_y}{\lambda_y - \lambda_x} = B + A \qquad \text{(AI-10)}$$

where $B = g\lambda_x X^o k_x$. Then:

$$\frac{A}{B} = \frac{k_y}{k_x} \cdot \frac{\lambda_y}{\lambda_y - \lambda_x} \qquad \text{(AI-11)}$$

and:

$$k_x = \frac{B}{A} \frac{k_y \lambda_y}{\lambda_y - \lambda_x} \cdot \qquad \text{(AI-12)}$$

$$k_x = \frac{(C')^o - (C'-C)^o}{(C'-C)^o} \cdot \frac{k_y \lambda_y}{(\lambda_y - \lambda_x)} \qquad \text{(AI-13)}$$

If a semilogarithmic plot of C against t is made, the quantities $(C')^o$ and $(C'-C)^o$ are easily obtained by graphical extrapolation. Since k_y was presumed known, k_x is obtained from Equation (AI-13).

APPENDIX II

In Section III of the text were obtained expressions for the number of atoms of species 1 and 2 present at the time of separation of 1 and 2, T units after the end of a bombardment of duration t, in terms of the independent rates of formation R, of 1 and 2. Species 2 is formed independently and by decay of species 1.

$$n_1 = \frac{R_1}{\lambda_1}(1-e^{-\lambda_1 t})e^{-\lambda_1 T} \qquad \text{(III-5)}$$

$$n_2 = \left(R_2 + \frac{\lambda_1}{\lambda_1-\lambda_2} R_1\right) \frac{(1-e^{-\lambda_2 t})e^{-\lambda_2 T}}{\lambda_2} - \frac{R_1}{\lambda_1-\lambda_2}(1-e^{-\lambda_1 t})e^{-\lambda_1 T} \qquad \text{(III-7)}$$

Let $\lambda_1 \gg \lambda_2$. For large T such that $e^{-\lambda_1 T} \longrightarrow 0$

$$n_2 = n_\infty = \frac{e^{-\lambda_2 T}(1-e^{-\lambda_2 t})}{\lambda_2}\left(R_2 + R_1 \frac{\lambda_1}{\lambda_1-\lambda_2}\right) \qquad \text{(AII-1)}$$

When T is not large, $n_2 = n_T$ given by Equation (III-7) above. Extrapolating the values obtained at time of separation back to the end of bombardment (multiplying by $e^{\lambda_2 T}$):

$$n_\infty^{\,o} = \frac{(1-e^{-\lambda_2 t})}{\lambda_2}\left[R_2 + R_1 \frac{\lambda_1}{\lambda_1-\lambda_2}\right] \qquad \text{(AII-2)}$$

$$n_T^{\,o} = \frac{(1-e^{-\lambda_2 t})}{\lambda_2}\left[R_2 + R_1 \frac{\lambda_1}{\lambda_1-\lambda_2}\right] - \frac{(1-e^{-\lambda_1 t})}{\lambda_2} R_1 \frac{\lambda_2}{\lambda_1-\lambda_2} e^{-(\lambda_1-\lambda_2)T} \qquad \text{(AII-3)}$$

$$n_\infty^{\,o} - n_T^{\,o} = R_1\left[\frac{e^{-(\lambda_1-\lambda_2)T}}{\lambda_1-\lambda_2}(1-e^{-\lambda_1 t})\right] \qquad \text{(AII-4)}$$

whence:

$$R_1 = \frac{(\lambda_1-\lambda_2)(n_\infty^{\,o} - n_T^{\,o})}{(1-e^{-\lambda_1 t})} e^{(\lambda_1-\lambda_2)T} \qquad \text{(AII-5)} \quad \text{(III-8)}$$

Substituting this value into Equation (AII-2), we obtain:

$$n_\infty^{\,o} = \frac{(1-e^{-\lambda_2 t})}{\lambda_2}\left[R_2 + \frac{\lambda_1 (n_\infty^{\,o} - n_T^{\,o}) e^{(\lambda_1-\lambda_2)T}}{(1-e^{-\lambda_1 t})} \right] \qquad \text{(AII-6)}$$

whence:

$$R_2 = \frac{\lambda_2 n_\infty^{\,o}}{(1-e^{-\lambda_2 t})} - \frac{\lambda_1 (n_\infty^{\,o} - n_T^{\,o}) e^{(\lambda_1-\lambda_2)T}}{(1-e^{-\lambda_1 t})} \qquad \begin{matrix}\text{(AII-7)} \\ \text{(III-9)}\end{matrix}$$

$$R_1 + R_2 = \frac{\lambda_2 n_\infty^{\,o}}{(1-e^{-\lambda_2 t})} + \frac{(n_\infty^{\,o} - n_T^{\,o}) e^{(\lambda_1-\lambda_2)T}}{(1-e^{-\lambda_1 t})} \left[\lambda_1 - \lambda_2 - \lambda_1 \right]$$

$$R_1 + R_2 = \lambda_2 \left\{ \frac{n_\infty^{\,o}}{(1-e^{-\lambda_2 t})} - \frac{(n_\infty^{\,o} - n_T^{\,o}) e^{(\lambda_1-\lambda_2)T}}{(1-e^{-\lambda_1 t})} \right\} \qquad \text{(AII-8)}$$

Since $R = IN\sigma$ by definition (cf., page 8), the ratio of formation cross sections is given by:

$$\frac{R_2}{R_1 + R_2} = \frac{\sigma_2}{\sigma_1 + \sigma_2} = \frac{n_\infty^{\,o}/(1-e^{-\lambda_2 t}) - (\lambda_1/\lambda_2)\,(n_\infty^{\,o} - n_T^{\,o}) e^{(\lambda_1-\lambda_2)T}/(1-e^{-\lambda_1 t})}{n_\infty^{\,o}/(1-e^{-\lambda_2 t}) - (n_\infty^{\,o} - n_T^{\,o}) e^{(\lambda_1-\lambda_2)T}/(1-e^{-\lambda_1 t})}$$

$$\frac{\sigma_2}{\sigma_1 + \sigma_2} = \frac{n_\infty^{\,o}(1-e^{-\lambda_1 t}) - (\lambda_1/\lambda_2)\,(n_\infty^{\,o} - n_T^{\,o})\,(1-e^{-\lambda_2 t}) e^{(\lambda_1-\lambda_2)T}}{n_\infty^{\,o}(1-e^{-\lambda_1 t}) - (n_\infty^{\,o} - n_T^{\,o})\,(1-e^{-\lambda_2 t}) e^{(\lambda_1-\lambda_2)T}} \qquad \text{(AII-9)}$$

This may be expressed in the form:

$$\frac{\sigma_2}{\sigma_1 + \sigma_2} = 1 - \left(\frac{\lambda_1 - \lambda_2}{\lambda_2}\right) \frac{(n_\infty^{\circ} - n_T^{\circ})\,(1-e^{-\lambda_2 t})e^{(\lambda_1-\lambda_2)T}}{n_\infty^{\circ}(1-e^{-\lambda_1 t}) - (n_\infty^{\circ} - n_T^{\circ})\,(1-e^{-\lambda_2 t})e^{(\lambda_1-\lambda_2)T}} \quad \begin{matrix}(AII\text{-}10)\\(III\text{-}10)\end{matrix}$$

For $\lambda_2 \ll \lambda_1$

$$\frac{\sigma_2}{\sigma_1 + \sigma_2} \simeq 1 - \left(\frac{\lambda_1}{\lambda_2}\right) \frac{(n_\infty^{\circ} - n_T^{\circ})\,(1-e^{-\lambda_2 t})e^{\lambda_1 T}}{n_\infty^{\circ}(1-e^{-\lambda_1 t}) - (n_\infty^{\circ} - n_T^{\circ})\,(1-e^{-\lambda_2 t})e^{\lambda_1 T}} \quad \begin{matrix}(AII\text{-}11)\\(III\text{-}11)\end{matrix}$$

APPENDIX III

Let us consider data which are of the following form: (1) the total yield of isobars of charge Z-1 or less; (2) the independent yield of the isobar of charge Z; and (3) the total yield of isobars of charge Z + n + 1 or greater, where n is the number of isobars not available for chemical separation, i.e., stable or short lived isobars. Let the area under the histogram be equal to unity. Now let us define a function E(X) such that

$$E(X) = \int_{X}^{+\infty} f(Z)dZ \qquad \text{(AIII-1)}$$

X being the abcissa with the center of the curve taken as the origin, X being expressed in units of the standard deviation of the curve. Then if we define Y as shown in Figure 6 (taking y as a positive number when in the direction shown), and the width of one block of the histogram (in X units) is a, our experimental data may be described as proportional to E(y), E(y-a) - E(y), and E(b).

We have prepared a master chart (shown in Figure 7) giving E(y)/E(y-a) as a function of Y for various a. From our experimental value for E(y)/E(y-a) one obtains from this chart a table giving y as a function of a. Now

$$|b| = (n + 1)a - |y|, \qquad \text{(AIII-2)}$$

so we have

$$y = f_1(a) \qquad \text{(AIII-3)}$$

and

$$b = f_2(a) \qquad \text{(AIII-4)}$$

therefore

$$E(y) = f_3(a) \qquad \text{(AIII-5)}$$

$$E(b) = f_4(a) \qquad \text{(AIII-6)}$$

therefore

$$E(b)/E(y) = f_5(a) \qquad \text{(AIII-7)}$$

but $E(b)/E(y)$ can be obtained from our experimental data. Equation (AIII-7), of the form $f_5(a)$ = constant, can then be solved by graphical means, giving a value for a, hence for y, and hence locating Z_o the center of the curve as

$$Z_o = Z - 1/2 + y/a \ . \qquad \text{(AIII-8)}$$

Since a histogram block has a width of 1 charge unit and a standard-deviation units, the standard deviation of the curve is $1/a$.

REFERENCES

1. R. H. Goeckermann and I. Perlman, Phys. Rev. 73, 1127 (1948), and Phys. Rev. 76, 628 (1949).
2. A. S. Newton, Phys. Rev. 75, 17 (1949).
3. J. Jungerman and S. C. Wright, Phys. Rev. 76, 1112 (1949).
4. P. R. O'Connor and G. T. Seaborg, Phys. Rev. 74, 1189 (1948).
5. I. Perlman, R. H. Goeckermann, D. H. Templeton, and J. J. Howland, Phys. Rev. 72, 352 (1947).
6. R. E. Batzel and G. T. Seaborg, Phys. Rev. 79, 528 (1950).
7. Y. Yamaguchi, Prog. Theor. Phys. 5, 143 (1950).
8. E. M. Douthett, private communication.
9. B. J. Finkle, E. J. Hoagland, S. Katcoff, and N. Sugarman, National Nuclear Energy Series, Plutonium Project Record, Vol. 9B, Div. IV, "Radiochemical Studies: The Fission Products," Paper No. 46 (McGraw-Hill Book Co., Inc., New York, 1951).
10. F. Suzor, Ann. phys. [12] 4, 269 (1949).
11. R. L. Aamodt, V. Petersen, and R. Phillips, private communication.
12. A. Ghiorso, A. H. Jaffey, H. P. Robinson, and B. B. Weissbourd, National Nuclear Energy Series, Plutonium Project Record, Vol. 14B, "The Transuranium Elements: Research Papers," Paper No. 16.8 (McGraw-Hill Book Co., Inc., New York, 1949).
13. E. Potter and H. Robinson, unpublished data.
14. L. R. Zumwalt, U. S. Atomic Energy Commission Declassified Document MDDC-1346 (February 8, 1949).
15. B. P. Burtt, Nucleonics 5, no. 2, 28-43 (1949).
16. L. Yaffe and K. M. Justus, J. Chem. Soc. (London), p. S341 (1949), Part V.

17. L. Malatesta, unpublished data.

18. W. Nervik and P. C. Stevenson, unpublished work.

19. M. Studier and R. James, unpublished data.

20. W. F. Biller, private communication.

21. W. W. Scott, "Standard Methods of Chemical Analysis," D. Van Nostrand Co., Inc., New York, 1939, Ed. 5, Vol. I, pp. 1058-9.

22. H. Hicks, private communication.

23. A. S. Newton, Thesis, University of Michigan, 1941.

24. G. Rudstam, P. C. Stevenson, and R. L. Folger, unpublished work.

25. G. T. Seaborg and I. Perlman, Revs. Modern Phys. 20, 585 (1948).

26. Chart of the Nuclides, General Electric Research Laboratory, 1950.

27. G. Wilkinson and H. G. Hicks, Phys. Rev. 75, 1370 (1949).

28. Ibid., 1687.

29. Ibid., 79, 815 (1950).

30. K. Street, Jr. and G. T. Seaborg, J. Am. Chem. Soc. 70, 4268 (1948).

31. E. R. Tompkins, U. S. Atomic Energy Commission Declassified Document AECD-1998 (October 31, 1947).

LIST OF ILLUSTRATIONS

Figure

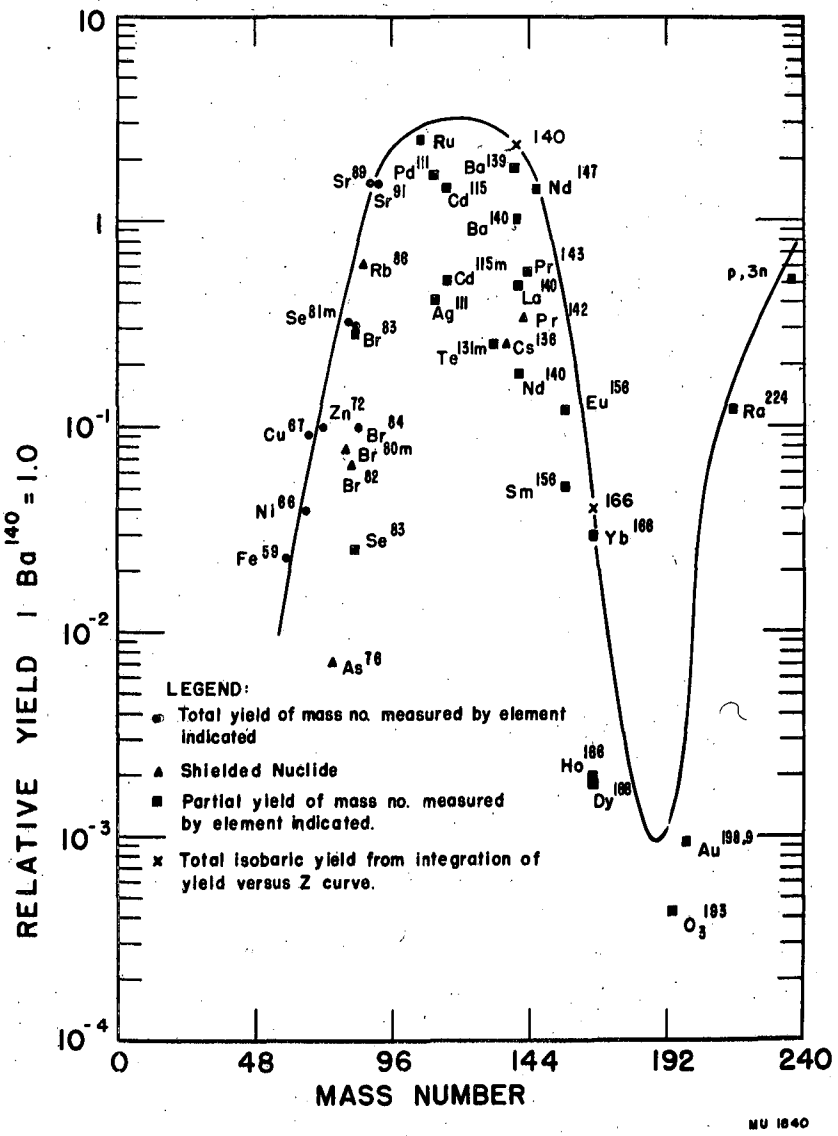
RELATIVE YIELD I Ba140 = 1.0
MASS NUMBER
LEGEND:
Total yield of mass no. measured by element indicated
Shielded Nuclide
Partial yield of mass no. measured by element indicated.
Total isobaric yield from integration of yield versus Z curve.
MU 1840

Fig. 1

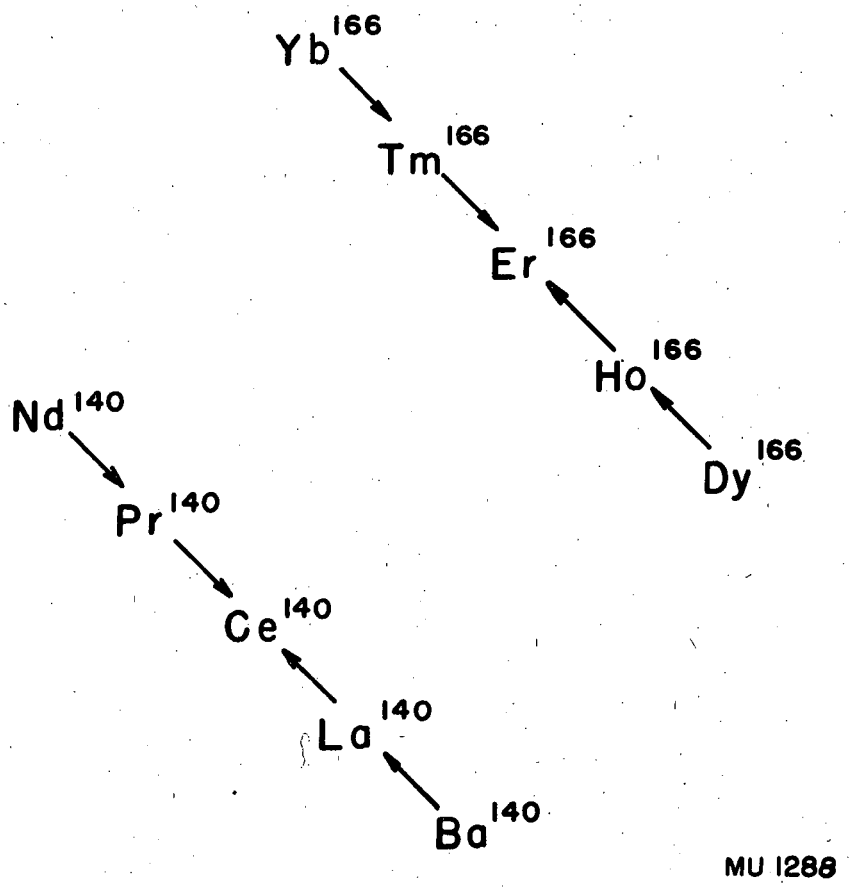
Yb 166
Tm 166
Er 166
Ho 166
Dy 166
Nd 140
Pr 140
Ce 140
La 140
Ba 140
MU 1288

Fig. 2

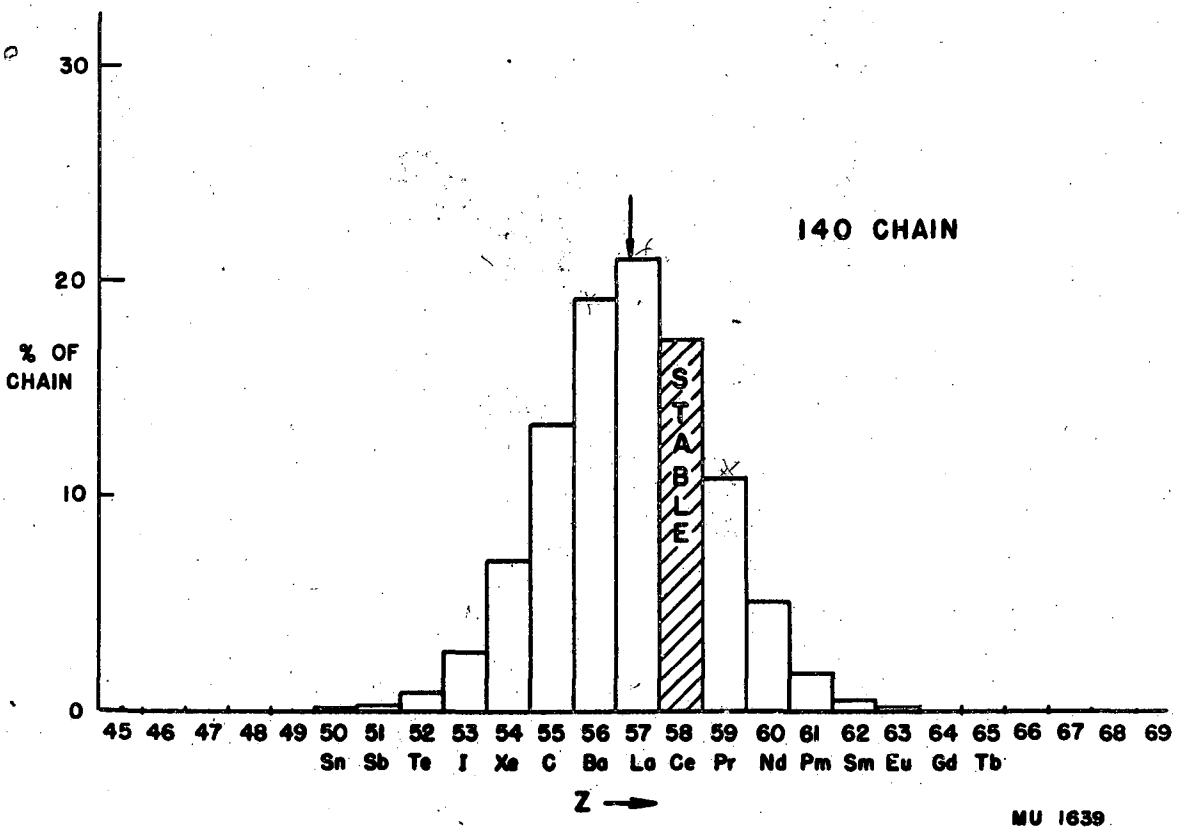
140 CHAIN
% OF CHAIN
30
20
10
0
STABLE
45 46 47 48 49 50 51 52 53 54 55 56 57 58 59 60 61 62 63 64 65 66 67 68 69
Sn Sb Te I Xe C Ba La Ce Pr Nd Pm Sm Eu Gd Tb
Z
MU 1639

Fig. 3

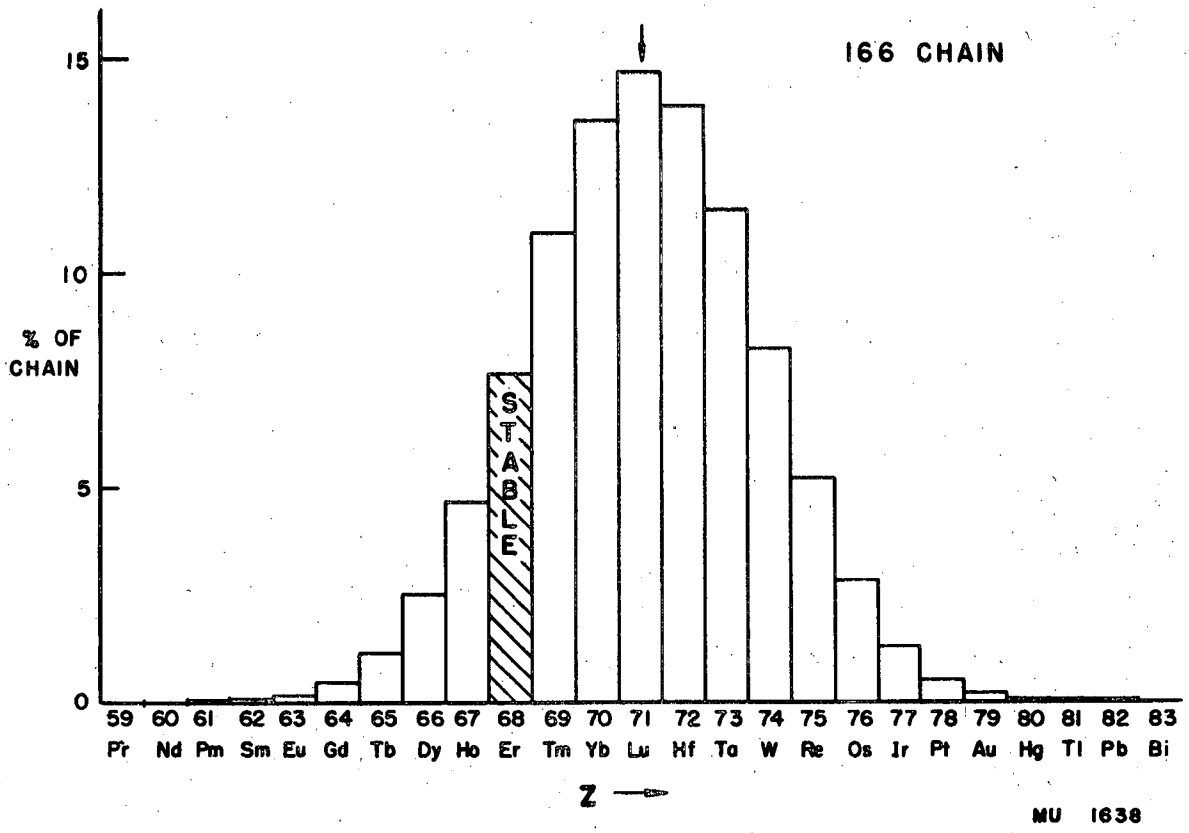
166 CHAIN
15
10
5
0
% OF CHAIN
STABLE
59 60 61 62 63 64 65 66 67 68 69 70 71 72 73 74 75 76 77 78 79 80 81 82 83
Pr Nd Pm Sm Eu Gd Tb Dy Ho Er Tm Yb Lu Hf Ta W Re Os Ir Pt Au Hg Tl Pb Bi
Z
MU 1638

Fig. 4

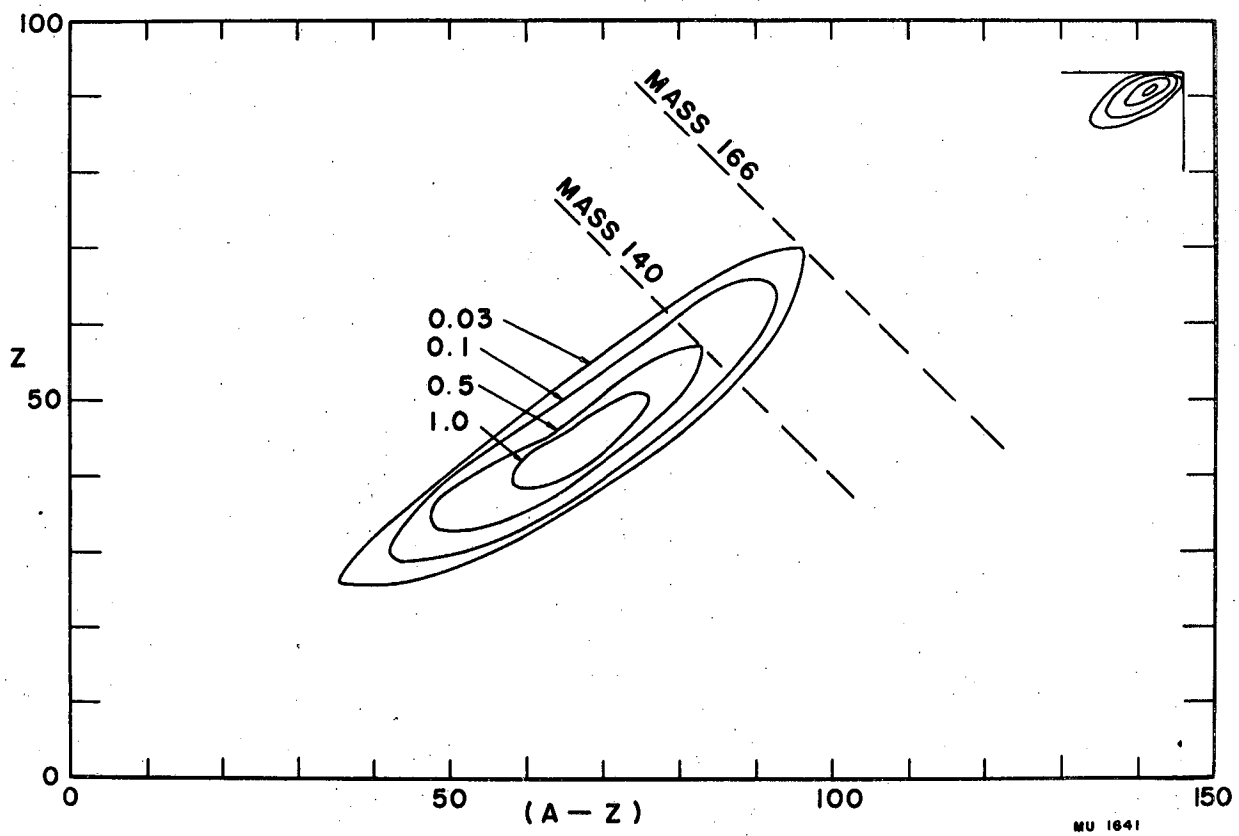

Fig. 5

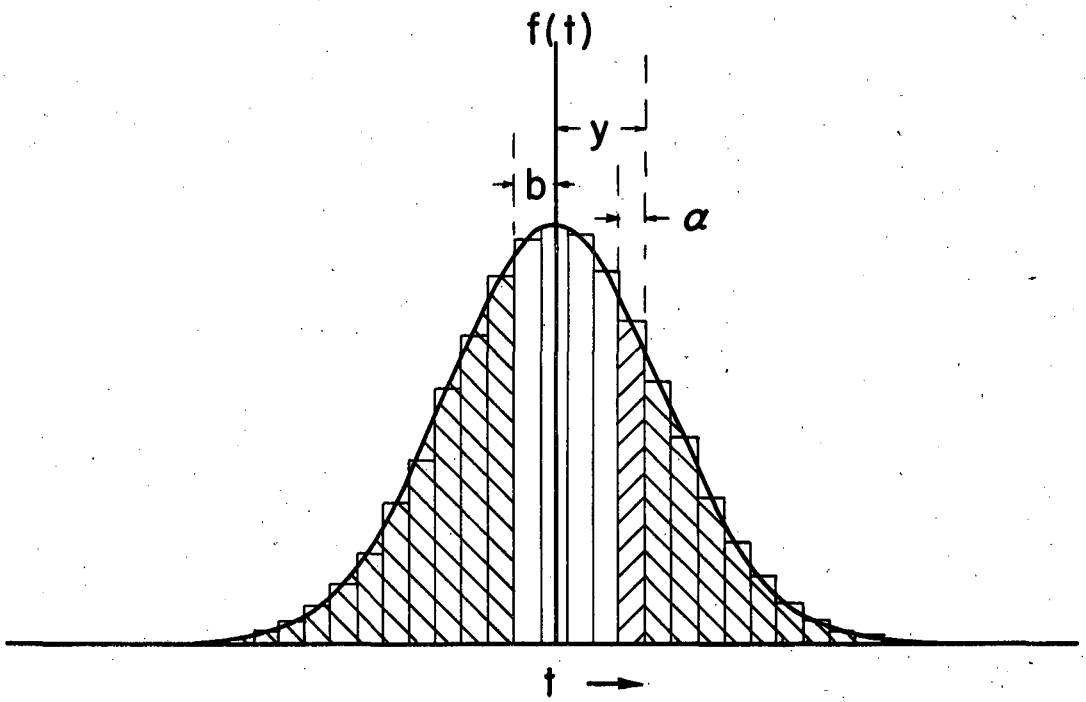

$$E(x) = \int_x^\infty f(t)\,dt$$

MU1287

Fig. 6

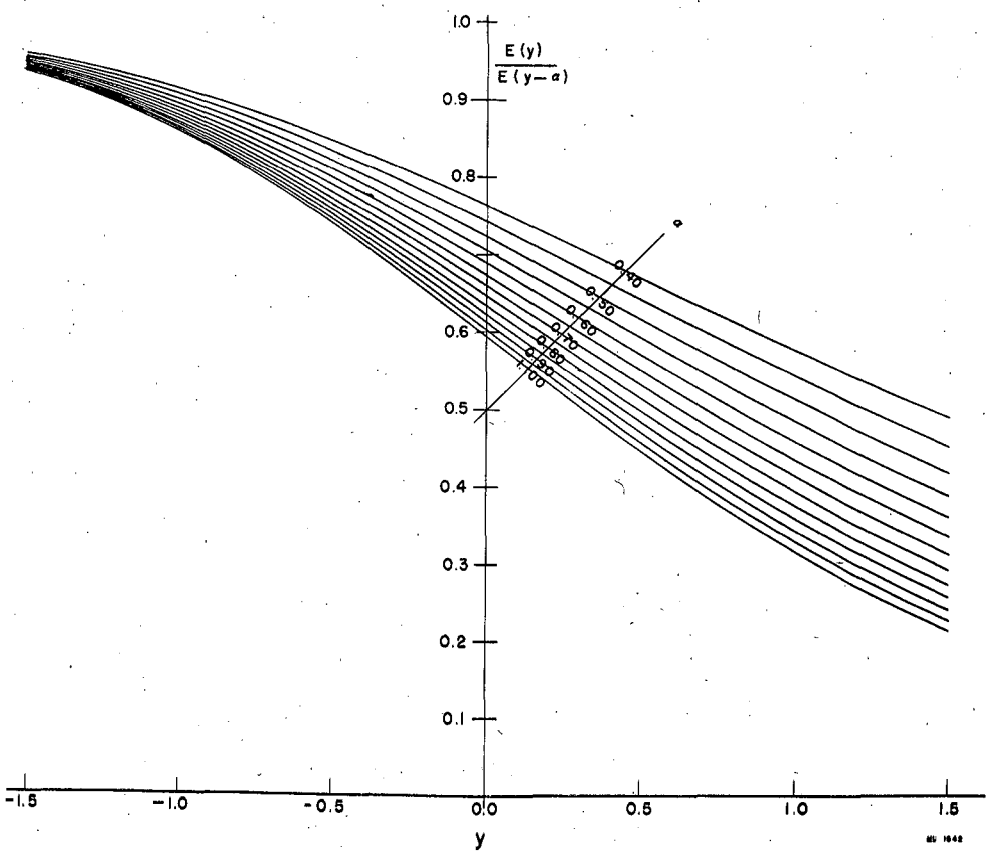

Fig. 7

UNCLASSIFIED